A rating curve model accounting for cyclic stage-discharge shifts due to seasonal aquatic vegetation

Emeline Perret, Benjamin Renard, Jérôme Le Coz

A rating curve model accounting for cyclic stage-discharge shifts due to seasonal aquatic vegetation

E. Perret [1], B. Renard [1], J. Le Coz [1]

[1]INRAE, UR RiverLy, F-69625, Villeurbanne, France

Key Points:

- A rating curve model accounting for aquatic vegetation was developed and estimated through Bayesian inference.
- Information on the vegetation development state should be used to estimate the rating curve.
- Discharge prediction in presence of aquatic plants was improved using the new model (relative errors decrease from ±50 % to ±20 %).

Corresponding author: Emeline Perret, `emeline.perret@inrae.fr`

Abstract

Managing stage-discharge relations at hydrometric stations affected by aquatic vegetation is challenging. Ratings vary continuously in time due to the plant development, which makes the streamflow time series difficult to predict. To the best of our knowledge, no rating curve model exists to deal with stations with a vegetated channel control, only manual adjustment methods. To address this issue, a temporal rating curve model accounting for transient changes due to vegetation is developed. The model is built on basic concepts from open-channel hydraulics and plant physiology. In the model, the flow resistance varies through time as a function of the plant development (growth and decay) and of the plant ability to reconfigure. Model parameters and uncertainty are estimated through Bayesian inference combining prior knowledge on the hydraulic controls at the station and observational data. In addition to the traditionally-used stage-discharge gaugings, the model allows the use of qualitative observations on the plant development state (e.g. no plant, growth, decay). The model is tested and validated for a French hydrometric station where frequent gaugings (twice a month) and written comments about vegetation are available over more than 20 years. Relative errors between the simulated discharges and the observed discharges mostly range between $\pm 20\,\%$ for the temporal rating curve. In contrast, they are higher than $\pm 50\,\%$ with a standard model with no vegetation module. This case study highlights the importance of using observations about plant development to predict water discharge. We finally discuss some possible improvements and extensions of the model and recommend methods for data collection.

1 Introduction

1.1 Rating curve management

Establishing the streamflow time series and its uncertainty is a priority for most hydrological studies and water management applications. The streamflow record is commonly computed by transforming a continuous water level record into water discharge using a stage-discharge relation, also known as a rating curve (World Meteorological Organization, 2010). Rating curves are site-specific and are usually built using occasional measurements of water discharge Q and stage h (i.e. gaugings), combined with information about hydraulic controls (section or channel controls) at the hydrometric station (Rantz, 1982). The process of building a rating curve is subject to a large uncertainty that needs to be quantified in order to make important water-related decisions (McMillan et al., 2017). Many methods exist to estimate rating curve uncertainty and have been applied with increasing frequency (Kiang et al., 2018).

One of the main problems for rating curve management is to deal with rating changes or "shifts" (Mansanarez et al., 2019). Indeed, stage-discharge relations are not always stable and can evolve in time, which leads to non-unique h-Q relations. Rating instabilities can be caused by sudden changes (e.g. morphological evolution induced by a flood, human constructions that affect the hydraulic control) and/or by transient changes (e.g. vegetation growth, accumulation of debris or ice). The challenge is to detect these changes and update the curve accordingly, e.g. modifying the rating curve model and/or re-estimating the model parameters. Some procedures exist to deal with sudden changes and are reported in Mansanarez et al. (2019). However, these methods are not suitable for transient changes due to aquatic vegetation. In that case, the stage-discharge relation varies continuously in time according to the vegetation evolution. Water discharge therefore needs to be estimated from the stage and other variables depending on time. To the best of our knowledge, no rating curve models accounting for aquatic vegetation exist in the literature.

In case of a section control, removing vegetation from the critical section (e.g. weir) is a frequent and common practice to avoid any effect of plants. This procedure is in general unrealistic in case of a channel control, because vegetation should be removed from

the entire controlling channel to totally cancel the plant effect at the station. In addition, it is considered as ecologically unacceptable in some countries and is hence forbidden or at least banned from actual practice. In case of channel controls, the rating curve shifts due to vegetation are generally not managed in real time, but instead are accounted for with manual and non-standardized methods, according to the station manager expertise. As far as we know, there exist no publications reviewing how different countries and hydrometric services actually manage these transient changes. For example, the French hydrometric services use a method called *corTH* that does not modify the base rating curve (BRC) derived with vegetation-free gaugings. Instead, it replaces the observed stage by a corrected stage that, once transformed by the BRC, leads to the estimated vegetation-affected discharge. This method is based on the assumption that the presence of plants leads to a temporary and overall translation of the stage-discharge relation. This approach heavily relies on gaugings to track the effect of vegetation in time. Such manual methods have many limitations, in particular because adjustments strongly rely on the expertise of the station manager. This expertise is in general poorly documented, making manual methods hardly reproducible. As a time-varying rating curve model that accounts for the hydraulic effects of seasonal aquatic vegetation is lacking, it is difficult to predict and keep track of actual changes in the stage-discharge relation.

1.2 Modelling flow/plant interactions

Many studies examined the flow-vegetation interactions in rivers at different scales (from the leaf, branch, plant, patch to the entire section) for diverse types of plants (rigid or flexible) and for diverse levels of submergence (submerged or emergent) with a focus on the effect of vegetation on the flow (Nikora, 2010; Folkard, 2011; Neary et al., 2012; Nepf, 2012; Luhar & Nepf, 2013; Albayrak et al., 2014). These studies indicate that aquatic vegetation induces a change in roughness, which modifies the flow resistance of a channel. Plants also act as obstacles that prevent water from flowing through the part of the channel cross-section that they occupy. When plant height and density increase, flow velocity decreases and channel resistance increases (Green, 2005).

Depending on the spatial scale of the study, the effect of the vegetation on the flow is either described by the drag force or by resistance coefficients such as the Darcy-Weisbach friction factor f_v [-] and the Manning coefficient n_v [$m^{-1/3}$.s] (Västilä & Järvelä, 2017; Shields et al., 2017). The resistance coefficients are generally preferred for stand-scale or reach-scale studies. Although it would be better to work with dimensionless Darcy-Weisbach friction factors, dimensional Manning coefficients are still widely used in practice and remain the most popular in hydraulic equations and in rating curve models.

Many formulae and look-up tables exist to evaluate the Manning coefficients of beds without aquatic vegetation. They are generally based on the grain size distribution of the bed surface material and other physical characteristics of a river (Meyer-Peter & Müller, 1948; Limerinos, 1970; Arcement & Schneider, 1989; Coon, 1998; Hicks & Mason, 1999). By contrast, few methods exist to estimate the Manning coefficient n_v related to the presence of plants (Petryk & Bosmajian, 1975; Fathi-Maghadam & Kouwen, 1997; Järvelä, 2004; Whittaker et al., 2013; Västilä & Järvelä, 2014; Shields et al., 2017). In addition, most of them were developed for floodplain vegetation, which does not necessarily have the same properties as in-stream vegetation. Some tabulated data are available in the literature (Chow, 1959; Barnes, 1967; Coon, 1998; Hicks & Mason, 1999; Fisher & Dawson, 2003) but they just enable evaluating n_v at a given time for a given density and type of vegetation. These classic tables cannot be used for estimating the hydraulic effects of plants through time.

Flow resistance equations for vegetated flows were historically developed for rigid plants using the analogy of the vertical rigid cylinder showing that the drag force applied to the cylinder increases with the squared average flow velocity (Petryk & Bosma-

jian, 1975; Pasche & Rouvé, 1985). However, they were not applicable in the case of natural rivers where the vegetation is often flexible. Models for flexible plants, or for a combination of rigid and flexible plants, were created subsequently (Järvelä, 2004; Whittaker et al., 2013; Västilä & Järvelä, 2014). A distinction between models for submerged and for emergent plants is also important. Indeed, depending on relative submergence, i.e. the ratio between the water depth and the height of the (deflected) plant H_p, the flow structure changes significantly within the reach (Vargas-Luna et al., 2015), so different parameterizations for the flow resistance equation need to be made (Wu et al., 1999; Shields et al., 2017; Västilä & Järvelä, 2017). In particular, the choice of a suitable flow velocity is crucial for evaluating the drag force generated by the plants and to calculate the resulting flow resistance (Västilä & Järvelä, 2017).

Most flow resistance equations relative to aquatic vegetation depend on the density of the plants over the channel section, their spatial distribution and their flexibility. Unfortunately, these equations were not developed from a practical and operational viewpoint (Aberle & Järvelä, 2013). The models require thorough knowledge of the plant characteristics, or measurements, that most often are not available at the stations (e.g. elasticity, size, age, growth rate). The plant flexibility is often used to model the ability of the plant to reconfigure under flow stress (Jalonen, 2015). Indeed, plants can align in the flow direction and bend to reduce their frontal area impacted by the flow and thus exert less resistance than if they were rigid (Kouwen & Fathi-Moghadam, 2000; de Langre, 2008). Vegetation density is often represented in models using the ratio between a characteristic reference area of vegetation, commonly defined as the frontal projected area of the plants perpendicular to the flow (A_p), and the ground area (A_b) occupied by the plants (Västilä et al., 2013). For leafy plants, the density is given by the Leaf Area Index: $LAI = A_L/A_b$, where A_L is the one-sided leaf area (leaves measured flat). However, information on the type of plant present on the riverbed is scarce at hydrometric stations, and measurements of plant development are also rare (e.g. no biomass samplings, no camera monitoring of the plant development, etc.). Hence, the literature models for n_v are too complex to use for operational purposes in hydrometry. It is nevertheless possible and valuable to organize measurement campaigns to estimate punctually the plant density in the channel, but it is difficult to monitor it continuously. A continuous-time model is therefore needed to describe plan development.

1.3 Modelling aquatic plant development in rivers

Numerous plant development models exist for terrestrial plants but fewer are available for aquatic plants (Carr et al., 1997; Adams et al., 2017). Some of them require a large number of parameters to be estimated. Others relate the growth rate to other variables, such as the water temperature, the incident radiation, the nutrients within the water and the dissolved oxygen. These measurements are rarely available at hydrometric stations (with the possible exception of water temperature).

Originally, growth and decay models for aquatic plants were developed for investigating vegetation development in lakes or reservoirs and problems of eutrophication (Asaeda et al., 2001; Hilton et al., 2006). Processes governing growth in lakes are partly similar to those in rivers, with the notable difference that plants in lakes are not subject to significant time-varying flows and drags (Hilton et al., 2006). In rivers, the light intensity and the water temperature are found to be the main driving factors for plant development (Carr et al., 1997). However, many models relate plant growth to water temperature only because temperature is easier to measure than irradiance (Yan & Hunt, 1999; Briére et al., 1999; van der Heide et al., 2006).

Plant development models relating growth rate to water temperature take a variety of mathematical forms: linear (Tollenaar et al., 1979), bi-linear (Olsen et al., 1993), multi-linear (Coelho & Dale, 1980), exponential (Room, 1986) and bell-shaped (Yin et

al., 1995; Yan & Hunt, 1999). Adams et al. (2017) tested 12 different growth rate-temperature models on tropical seagrass species and found that the bell-shaped model of Yan & Hunt (1999), which is a simplified version of the model of Yin et al. (1995), was the most accurate. This model best fits the data presented in Adams et al. (2017) and has biologically-meaningful parameters, such as: the base temperature that triggers plant growth, the optimal temperature inducing the maximal growth rate and the ceiling temperature that marks the end of growth and the beginning of the plant decay. Following the growth rate-temperature model of Yin et al. (1995), Yin et al. (2003) propose a bell-shaped temporal equation for modelling plant growth using characteristic times of the plant growth cycle only. The Yin et al. (2003) model is derived from biological concepts and based on the assumption that the plant development can be described according to the seasons, i.e. to the time during the year. The underlying assumption is that the season evolution reflects the evolution of key forcings such as irradiance and water temperature. The bell-shaped form accounts for slow growth at the beginning of the plant development and close to the growth end time. This model is attractive for operational purposes as it uses time directly, rather than some additional physical parameters, which are not always measured at hydrometric stations.

1.4 Objectives

The main objective of this paper is to develop a temporal rating curve model for channel controls built on both hydraulic and biological concepts in order to better compute discharge at hydrometric stations affected by seasonal aquatic vegetation. The model is intended to be used for operational purposes and hence only relies on information that can be easily retrieved at hydrometric stations. Specific objectives also include: (i) assessing the relative importance of various model components such as those related to vegetation growth/decay and plant reconfiguration and (ii) highlighting useful observations (e.g. gaugings and information on vegetation development) that improve the estimation of the rating curve.

The rest of the paper is organized as follows. Section 2 presents the formulation of the temporal rating curve model that accounts for the presence of seasonal aquatic vegetation. Section 3 describes the Bayesian approach used to estimate the model parameters using prior knowledge on the hydraulic controls at the station and observational data (hydraulic gaugings and vegetation observations). The uncertainties of both sources of information are included. In Section 5, the model performance is tested using data from a French hydrometric station presented in Section 4 for which frequent measurements are available. Sensitivity tests are also carried out to assess the importance of the reconfiguration effect in the model and of having observations about plant development for its estimation. Finally, Section 6 discusses the results and limitations of the model and presents some suggestions for improving it.

2 Formulation of the rating curve model

2.1 Hydraulic basis

The rating curve model for channel controls is constructed considering that vegetation essentially induces channel roughness changes, which modifies the flow resistance. Vegetation dissipates flow energy through a multitude of mechanisms, such as by waving in the flow or by simply blocking the flow. At the channel cross-section scale, the resulting effect of those processes can be lumped into one single resistance coefficient (e.g. Manning coefficient).

The model can be used at hydrometric stations fulfilling the following conditions:

1. The stage-discharge relation is governed by a channel control that can be assimilated to a wide rectangular channel; section controls (e.g. rectangular weir) are not explored because, in those cases, the stage-discharge relation does not depend on bed roughness (Rantz, 1982). The effect of vegetation, if it exists, should be taken into account in another way than with a roughness change.
2. The in-stream vegetation is made of rigid or flexible macrophytes that are just-submerged (i.e. the height of deflected plant equals the water depth) or not deeply submerged (i.e. the relative submergence can be slightly greater than 1 but stays close to 1). The cases of emergent plants and plants staying deep and close to the bed are excluded.
3. The wetted area reduction by the plants from the bank or from the bed is negligible. The channel width is not reduced by plants growing from the bank and the flow is not obstructed by a dense and permanent vegetative cover on the main channel bed.
4. The spatial distribution of the in-stream vegetation is quite homogeneous at the station.

The standard form of a rating curve for a given hydraulic control is a power equation (Rantz, 1982; World Meteorological Organization, 2010; Mansanarez, 2016). In case of a wide and rectangular channel control, the rating curve model is generally derived from the Manning-Strickler equation, expressed as follows (Le Coz et al., 2014):

$$\begin{cases} Q(h,\tau) = \dfrac{1}{n(\tau)} B \sqrt{S_0} [h(\tau) - b]^c \text{ for } h > b \\ Q(h,\tau) = 0 \text{ for } h \leq b \end{cases} \tag{1}$$

with Q the discharge, h the stage, τ the time, n the total flow resistance coefficient, B the channel width, S_0 the bed slope (approximating the energy slope in the case of a uniform flow), b the offset of the control (i.e. in our case the bottom level of the channel) and $c = 5/3$ the exponent related to the wide rectangular channel control. This kind of standard power-law rating curve can be used for modeling a single channel control affected by aquatic vegetation provided that temporal roughness variations are assessed.

The Manning-Strickler equation has the advantage to take into account the total flow resistance through the total Manning coefficient n. The total flow resistance is commonly decomposed into several resistance contributions with different and additive coefficients (Cowan, 1956): the resistance due to bed material, to bed irregularity, to channel geometrical variations, to obstacles in the channel and the resistance due to vegetation. The resistance component related to vegetation ($n_v(\tau)$) is the most likely to vary in time and the one that has the strongest temporal effect on the total flow resistance (Coon, 1998). A simplified decomposition of the total flow resistance is often adopted in flow-vegetation interaction studies (Morin et al., 2000):

$$n^2(\tau) = n_b^2 + n_v^2(\tau) \tag{2}$$

where n_b is the Manning coefficient of the bed without vegetation (or at least with vegetation that do not evolve over the years) and $n_v(\tau)$ is the Manning coefficient related to the presence of aquatic vegetation varying in time τ. Equation 2 comes from the linear superposition principle for Darcy-Weisbach friction factors f (Aberle & Järvelä, 2013) simply converted into Manning coefficients n as follows (Smart et al., 2002):

$$n^2 = \frac{f R_h^{1/3}}{8g} \tag{3}$$

where g is the gravity acceleration (9.81 m/s^2) and R_h is the hydraulic radius, which can be approximated by flow depth $(h - b)$ in the case of a wide rectangular channel.

Combining Morin's decomposition of flow resistance (Equation 2) with Equation 1, the actual discharge can be written as a product of a base discharge Q_0 not affected

by the vegetation and a correction factor reflecting the effect of vegetation on the channel roughness:

$$\begin{cases} Q(h,\tau) = Q_0(h,\tau)\left(1+\dfrac{n_v^2(\tau)}{n_b^2}\right)^{-1/2} & \text{for } h > b \\ Q(h,\tau) = 0 \text{ for } h \leq b \end{cases} \tag{4}$$

with:

$$Q_0(h,\tau) = \frac{B\sqrt{S_0}}{n_b}[h(\tau)-b]^c \tag{5}$$

2.2 Flow resistance induced by aquatic vegetation

After a literature review, the physically-based flow resistance equation of Järvelä (2004) is chosen for computing $n_v(\tau)$ because it was developed for similar conditions than those presented in Section 2.1. This equation was initially created for riparian vegetation and is suitable for modeling flow resistance related to flexible (or rigid) just-submerged or emergent plants over a channel cross-section, assuming a homogeneous spatial distribution of the plants. The Järvelä (2004) equation expresses the Darcy-Weisbach flow resistance coefficient f_v relative to vegetation as follows:

$$f_v(\tau) = 4C_{D_\chi} LAI(\tau)\left(\frac{U_c(\tau)}{U_\chi}\right)^\chi \tag{6}$$

with LAI the Leaf Area Index, C_{D_χ} the species-specific drag coefficient, χ the species-specific reconfiguration exponent also called the Vogel exponent, U_c the characteristic flow velocity and U_χ the lowest velocity used in determining χ (in other words a velocity that scales U_c). Equation 6 takes into account the plant density over the cross-section (mainly through the LAI parameter) as well as the plant ability to reconfigure under flow power using $(U_c(\tau)/U_\chi)^\chi$ (i.e. plant bending and streamlining). The coefficient χ was evaluated using laboratory experiments for several plant species (Järvelä, 2004; Västilä & Järvelä, 2014, 2017). For a rigid plant, $\chi = 0$ and a leafy flexible plant has a χ equal to around -1, typically.

We extend the applicability of the Järvelä (2004) equation to in-stream plants that are not deeply submerged, by assuming that the water volume flowing over the vegetated part of the cross-section is negligible. Then, the vegetation induces a drag all over the water column.

According to Järvelä (2004), Equation 6 can readily be used for engineering applications. An operational procedure has been proposed for calculating f_v (Västilä & Järvelä, 2017). However in practice, continuously monitoring the evolution of $LAI(\tau)$ remains a difficult task. In addition, these measurements are not common at hydrometric stations, nor is the evaluation of the type of plants present on the riverbed. Equation 6 is thus too complex for our purpose and therefore needs to be simplified. The Järvelä (2004) model can be seen as a combination of two functions: one describing the impact of the plant development (growth, increase in density, etc.) and one characterising the effect of plant reconfiguration:

$$f_v(\tau) = d(\tau) \times \left(\frac{U_m(\tau)}{U_\chi}\right)^\chi \tag{7}$$

where $d(\tau) = 4C_{D_\chi} LAI(\tau)$ is a function describing the hydraulic resistance due to the plant development cycle (growth and decay) and $(U_m(\tau)/U_\chi)^\chi$ is a function characterizing the plant reconfiguration. Note that in case of just-submerged or not deeply submerged plant, the characteristic velocity U_c can be assimilated to the mean velocity U_m. The function $d(\tau)$ is seen as a proxy of the plant biomass evolution and could be modeled using an empirical temporal equation not relying on $LAI(\tau)$, as will be described in the next section.

It is important to note that the plant is able to bend and/or align in the flow direction only when the mean velocity U_m exceeds a minimum velocity U_χ. Below this value, the reconfiguration should not be taken into account, so the reconfiguration function needs to be set to 1. This condition is formally added in the flow resistance equation:

$$f_v(\tau) = d(\tau) \times \min\left\{\left(\frac{U_m(\tau)}{U_\chi}\right)^\chi ; 1\right\} \tag{8}$$

Going from f_v to n_v using Equation 3 and replacing the mean velocity U_m by the discharge Q divided by the wetted area $B[h(\tau) - b]$, the time-varying Manning coefficient related to vegetation is finally expressed as follows:

$$n_v^2(\tau) = \frac{d(\tau)[h(\tau) - b]^{1/3}}{8g} \min\left\{\left(\frac{Q(\tau)}{U_\chi B[h(\tau) - b]}\right)^\chi ; 1\right\} \tag{9}$$

2.3 Model for plant development

The proxy $d(\tau)$ is assumed to evolve over time in a similar way as the biomass $w(\tau)$. Therefore, a model for plant development (biomass growth and decline) is used to estimate $d(\tau)$. Remember that $d(\tau)$ and $w(\tau)$ cannot be compared in terms of values, just in terms of temporal evolution.

We first need to introduce the shorthand notation t to represent the within-year time, i.e. the time within the cycle of plant development. If the time τ is expressed in years, then t is simply the fractional part of τ, varying between zero and one from an arbitrary start date in the year. If possible, the start date should be chosen under the guidance of experts in aquatic plants (i.e. according to the plant species and its development cycle). In this paper, it is fixed to January 1^{st}. The growth rate temporal model of Yin et al. (2003) is chosen for modelling the plant biomass evolution $w(t)$ within a year (see Figure 1):

$$\frac{dw}{dt} = GR_{max}\left(\frac{t_e - t}{t_e - t_m}\right)\left(\frac{t - t_b}{t_m - t_b}\right)^{\frac{t_m - t_b}{t_e - t_m}} \tag{10}$$

with dw/dt the growth rate, t_b the time at which the plant begins to grow, t_m the time at which the growth rate is maximum, t_e the time corresponding to the end of the growth and the beginning of plant decline, and GR_{max} the maximal growth rate. The Yin et al. (2003) model has a unimodal bell-shaped form like the usual growth rate models taking water temperature as input instead of time. In the Yin et al. (2003) study, t_b is assumed equal to zero, meaning that the plant start to grow at the beginning of the year. We do not make this assumption here.

Integrating Equation 10 and assuming the maximum of biomass w_{max} is reached at $t = t_e$ leads to the following equation for $w(t)$ (see Appendix A for details):

$$\begin{cases} w(t) = w_{max}\left(\dfrac{t - t_b}{t_e - t_b}\right)^{\frac{t_e - t_b}{t_e - t_m}}\left[\dfrac{2t_e - t_m - t}{t_e - t_m}\right] & \text{for } t_b < t < t_f \\ w(t) = 0 \text{ otherwise} \end{cases} \tag{11}$$

Before t_b, nothing grows and the biomass is set to zero. After $t = t_e$, the growth rate dw/dt becomes negative, which corresponds to the beginning of the biomass decline. Once the final time $t_f = 2t_e - t_m$ is reached, the biomass is fixed to 0 to avoid having negative biomass. The time t_f marks the end of the plant cycle.

The model illustrated in Figure 1 describes a kind of vegetation which completely disappears at the end of its growth cycle. Plants that live through the dormant period are not considered. Their effect on flow can be included in the constant Manning coefficient n_b in our rating curve model. Note also that Equation 11 does not account for

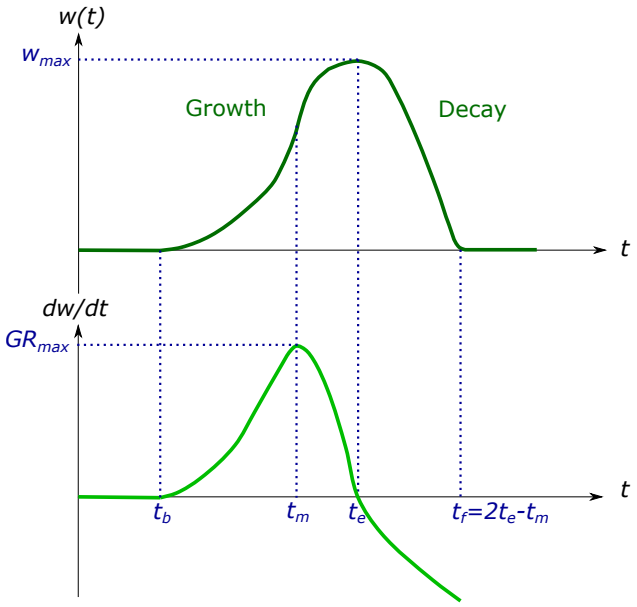

Figure 1: Evolution of the biomass $w(t)$ (Equation 11) and of the growth rate dw/dt (Equation 10) with characteristic times. See text for definition of variables.

external perturbations (e.g. flood, sudden drop in water temperature, changes in nutrient loads) that can impact the plant development and change its cyclic shape. These important factors will be discussed later in the section 6.3, but for the rating curve model we choose to keep this cyclic approach (Figure 1).

The plant development model depends on parameters t_b, t_m, t_e and w_{max} only. Keeping these parameters constant from year to year implies that the vegetation cycle is exactly the same every year. This assumption is too restrictive. Consequently, these parameters are allowed to vary from year to year in the model. The case study will explore this issue in more depth and will evaluate whether at least some of these parameters can reasonably be fixed.

2.4 The final rating curve model

The final rating curve model is expressed using a proxy $d(\tau)$ for time-varying plant biomass:

$$\begin{cases} Q(h,\tau) = Q_0(h,\tau)\left[1 + \dfrac{d(\tau)[h(\tau)-b]^{1/3}}{8gn_b^2}\min\left\{\left(\dfrac{Q(h,\tau)}{U_\chi B[h(\tau)-b]}\right)^{\chi};1\right\}\right]^{-1/2} & \text{for } h > b \\ Q(h,\tau) = 0 \text{ for } h \leq b \end{cases} \quad (12)$$

with:

$$d(\tau) = d_{max}\left(\frac{t-t_b}{t_e-t_b}\right)^{\frac{t_e-t_b}{t_e-t_m}}\left[\frac{2t_e-t_m-t}{t_e-t_m}\right] = d_{max}d_0(\tau) \quad (13)$$

where $Q_0(h,\tau)$ is the stage-discharge relation not affected by the presence of vegetation (see Equation 5), d_{max} is the maximal proxy biomass and $d_0(\tau)$ is the dimensionless time-varying component of $d(\tau)$. In practice, the discharge time series can be estimated from Equation 12 using the stage time series $h(\tau)$ and the plant evolution $d(\tau)$ deduced from Equation 13.

No explicit solution exists for Equation 12 because the discharge Q is present on both sides of the equation. Nevertheless, Equation 12 can be rewritten in a polynomial form by squaring both sides and then solved using the Newton-Raphson algorithm:

$$Q^2 + \gamma_1 \min\left\{\frac{Q^\chi}{\gamma_2}; 1\right\} Q^2 - Q_0^2 = 0 \tag{14}$$

with:

$$\gamma_1 = \frac{d(\tau)[h(\tau) - b]^{\frac{1}{3}}}{8gn_b^2} \tag{15}$$

$$\gamma_2 = U_\chi^\chi B^\chi [h(\tau) - b]^\chi \tag{16}$$

For mathematical convenience, the reconfiguration coefficient χ ranges between 0 and -2 (i.e. same range as in Vogel (1994) according to Luhar & Nepf (2013)). This limitation is reasonable regarding the values found for χ in literature, i.e. varying around -1 (Västilä & Järvelä, 2014), and ensures that Equation 14 has a unique solution.

The model is generic but needs to be estimated using local information. It can be applied to any stations that comply with the conditions presented in Section 2.1, for instance using the code released with this paper (see Data availability statement).

3 Bayesian inference

3.1 Extending the model to return the vegetation state

The final rating curve model of Equation 12 requires computing the dimensionless time series $d_0(\tau) = d(\tau)/d_{max}$, which can be interpreted as a dimensionless indicator of the vegetation development state at time τ (Figure 2a): $d_0(\tau) = 0$ means that there is no vegetation; $d_0(\tau) = 1$ denotes the vegetation peak; $0 < d_0(\tau) < 1$ corresponds to vegetation growth (before t_e) and decline (after t_e). Extending the model to return the vegetation state will allow to use vegetation observations as estimation data, by comparing the observed vegetation state with the one simulated by the model through $d_0(\tau)$. To do so, two steps are required in practice, as described next.

The first step is to convert $d_0(\tau)$ into an angle $\eta(\tau)$ of values comprised between 0 and 2π (Figure 2b). This procedure is done to distinguish more readily between the growth ($\eta < \pi$) and the decline ($\eta > \pi$) stages. Formally:

$$\begin{cases} \eta(\tau) = \pi d_0(\tau) \text{ if } t \leq t_e \\ \eta(\tau) = 2\pi - \pi d_0(\tau) \text{ if } t > t_e \end{cases} \tag{17}$$

The second step is to extend the rating curve model of Equation 12 so that it returns this angle, in addition to discharge. Because handling circular variables such as angle η requires specific care, it is more convenient to return its sine and cosine. Consequently, the model to be estimated can be viewed as a model with two inputs (stage h and time τ) and three outputs (discharge $\hat{Q}$, $\cos(\hat{\eta})$ and $\sin(\hat{\eta})$), as formalized below:

$$\boldsymbol{\mathcal{M}}(h, \tau; \boldsymbol{\theta}) = \begin{pmatrix} \hat{Q}(h, \tau; \boldsymbol{\theta}) \\ \cos(\hat{\eta}(\tau; \boldsymbol{\theta})) \\ \sin(\hat{\eta}(\tau; \boldsymbol{\theta})) \end{pmatrix} \tag{18}$$

Equation 18 makes the unknown parameters $\boldsymbol{\theta} = (B, S_0, n_b, b, c, \chi, U_\chi, \boldsymbol{t_b}, \boldsymbol{t_m}, \boldsymbol{t_e}, \boldsymbol{d_{max}})$ to be inferred explicit. The components of the $\boldsymbol{t_b}$, $\boldsymbol{t_m}$, $\boldsymbol{t_e}$, $\boldsymbol{d_{max}}$ vectors are year-specific

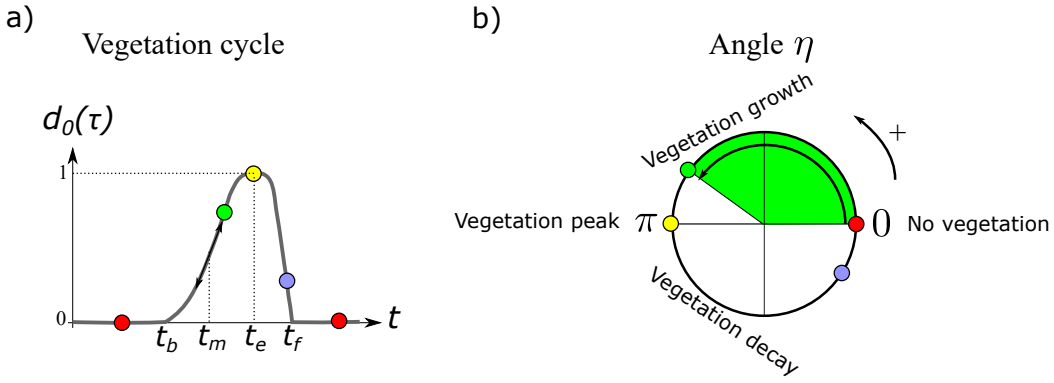

Figure 2: Interpretation of the dimensionless biomass proxy $d_0(\tau)$ as a position within the vegetation cycle (a) and its translation in terms of an angle η (b).

so for each year these components are estimated. The first output is obtained by applying Equation 12; the second and third outputs are obtained by first applying Equation 13 to compute $d_0(\tau)$, then by transforming it into angle $\hat{\eta}(\tau)$ through Equation 17.

3.2 Inference setup and assumptions

Let $\left(\widetilde{\tau}_i, \widetilde{h}_i, \widetilde{Q}_i, \cos(\widetilde{\eta}_i), \sin(\widetilde{\eta}_i)\right)_{i=1:M}$ denote the observational data used to estimate the model $\boldsymbol{\mathcal{M}}$. Estimation data are vectors comprising all input/output variables of model $\boldsymbol{\mathcal{M}}$. The vector can further be interpreted as a "traditional" gauging $\left(\widetilde{h}_i, \widetilde{Q}_i\right)$ augmented with a vegetation observation $(\widetilde{\tau}_i, \cos(\widetilde{\eta}_i), \sin(\widetilde{\eta}_i))$. Note that the vegetation observation can be derived from a qualitative assessment of the vegetation state. Importantly, it may be uncertain, so that it can accommodate more or less vague statements as shown in Table 1.

Table 1: Correspondence between qualitative assessments of the vegetation state and the vegetation observations used for model estimation.

Statement	angle $\widetilde{\eta}_i$	$\cos(\widetilde{\eta}_i)$	$\sin(\widetilde{\eta}_i)$
1/ there is no vegetation	0 ± 0	1 ± 0	0 ± 0
2/ there are few developing plants	$\pi/4 \pm \pi/4$	0.5 ± 0.5	0.5 ± 0.5
3/ there is vegetation, and the vegetation cycle is in its growing stage	$\pi/2 \pm \pi/2$	0 ± 1	0.5 ± 0.5
4/ there is vegetation, and the vegetation cycle is in its decaying stage	$3\pi/2 \pm \pi/2$	0 ± 1	-0.5 ± 0.5

Note: depending on the statement details, these values can be reviewed and their associated uncertainty can be adjusted.

The following assumptions are made to relate estimation data to the model predictions:

$$\begin{cases} \widetilde{Q}_i = \hat{Q}\left(\widetilde{h}_i, \widetilde{\tau}_i; \boldsymbol{\theta}\right) + \delta_{Q,i} + \varepsilon_{Q,i} \\ \cos(\widetilde{\eta}_i) = cos\left(\hat{\eta}(\widetilde{\tau}_i; \boldsymbol{\theta})\right) + \delta_{cos,i} + \varepsilon_{cos,i} \\ \sin(\widetilde{\eta}_i) = sin\left(\hat{\eta}(\widetilde{\tau}_i; \boldsymbol{\theta})\right) + \delta_{sin,i} + \varepsilon_{sin,i} \end{cases} \tag{19}$$

This equation states that for each output variable, the observed value is equal to the corresponding value simulated by the model plus an observation error $\delta_{.,i}$ plus a structural error $\varepsilon_{.,i}$. All errors are assumed to be mutually independent, and the following probabilistic assumptions are made:

$$\begin{cases} \delta_{Q,i} \sim \mathcal{N}(0, u_{Q,i}) \ ; \ \varepsilon_{Q,i} \sim \mathcal{N}(0; \gamma_{Q,1} + \gamma_{Q,2}\hat{Q}_i) \\ \delta_{cos,i} \sim \mathcal{N}(0, u_{cos,i}) \ ; \ \varepsilon_{cos,i} \sim \mathcal{N}(0; \gamma_{cos}) \\ \delta_{sin,i} \sim \mathcal{N}(0, u_{sin,i}) \ ; \ \varepsilon_{sin,i} \sim \mathcal{N}(0; \gamma_{sin}) \end{cases} \tag{20}$$

For each output variable, the standard deviation $u_{.,i}$ is assumed to be known and may vary between observations. This standard deviation quantifies measurement uncertainty and should ideally be specified following an uncertainty analysis of the measurement process (see Le Coz et al., 2014, for more details). Conversely, the standard deviation of structural errors is more difficult to specify before model estimation even though reasonable bounds can be defined; it is therefore assumed to be unknown and is inferred along with model parameters $\boldsymbol{\theta}$. Note that for the discharge output, the standard deviation of structural errors is allowed to increase linearly with the simulated discharge; this is made to account for the frequently-observed fact that structural uncertainty of rating curves tends to increase with the simulated discharge (Mansanarez et al., 2019). Conversely, the standard deviation of structural errors is assumed to be constant for the sine and cosine outputs.

3.3 Posterior distribution

Due to the mutual independence assumption for all error terms in Equation 19, the likelihood resulting from the assumptions discussed in the previous section can be computed as follows:

$$\begin{aligned} & p\left(\widetilde{\boldsymbol{Q}}, \cos(\widetilde{\boldsymbol{\eta}}), \sin(\widetilde{\boldsymbol{\eta}}) \mid \boldsymbol{\theta}, \boldsymbol{\gamma}, \widetilde{\boldsymbol{\tau}}, \widetilde{\boldsymbol{h}}\right) = \\ & \prod_{i=1}^{M} \phi\left(\widetilde{Q}_i; \hat{Q}\left(\widetilde{h}_i, \widetilde{\tau}_i; \boldsymbol{\theta}\right), \sqrt{u_{Q,i}^2 + \left(\gamma_{Q,1} + \gamma_{Q,2}\hat{Q}_i\right)^2}\right) \\ & \times \prod_{i=1}^{M} \phi\left(\cos(\widetilde{\eta}_i); \cos\left(\hat{\eta}(\widetilde{\tau}_i; \boldsymbol{\theta})\right), \gamma_{\cos}\right) \\ & \times \prod_{i=1}^{M} \phi\left(\sin(\widetilde{\eta}_i); \sin\left(\hat{\eta}(\widetilde{\tau}_i; \boldsymbol{\theta})\right), \gamma_{\sin}\right) \end{aligned} \tag{21}$$

where $\phi(z; m, s)$ is the probability density function (pdf) of a Gaussian distribution $\mathcal{N}(m, s)$ with mean m and standard deviation s evaluated at z. Note that the multiplicative nature of this likelihood makes the handling of missing data straightforward: corresponding terms can simply be omitted in the product of Equation 21.

Based on Bayes theorem, this likelihood can be combined with a prior pdf on unknown parameters, $p(\boldsymbol{\theta}, \boldsymbol{\gamma})$, to yield the following posterior pdf:

$$p\left(\boldsymbol{\theta}, \boldsymbol{\gamma} \mid \widetilde{\boldsymbol{Q}}, \cos(\widetilde{\boldsymbol{\eta}}), \sin(\widetilde{\boldsymbol{\eta}}), \widetilde{\boldsymbol{\tau}}, \widetilde{\boldsymbol{h}}\right) \propto p\left(\widetilde{\boldsymbol{Q}}, \cos(\widetilde{\boldsymbol{\eta}}), \sin(\widetilde{\boldsymbol{\eta}}) \mid \boldsymbol{\theta}, \boldsymbol{\gamma}, \widetilde{\boldsymbol{\tau}}, \widetilde{\boldsymbol{h}}\right) \times p(\boldsymbol{\theta}, \boldsymbol{\gamma}) \tag{22}$$

Note that the specification of prior distributions is case-specific and will be further discussed in the case study. Guidelines and examples related to the Bayesian method used here can also be found in Le Coz et al. (2014); Lundquist et al. (2016); Horner et al. (2018); Mansanarez et al. (2019).

3.4 MCMC sampling

The posterior pdf of Equation 22 is explored by means of a Markov Chain Monte Carlo (MCMC) sampler, described in Renard et al. (2006). In this paper a total of 100,000 MCMC iterations are performed. The first half is discarded as a burn-in period, and the remaining iterations are further thinned by a factor of 10; this implies that subsequent computations are based on a MCMC subsample of size 5,000, which is sufficient to achieve an acceptable accuracy while avoiding storage and computing time issues. MCMC convergence is checked by visualising all MCMC traces.

4 Study case

4.1 The Ill River at Ladhof, France

The Ladhof hydrometric station is located on the Ill River in Colmar, East France, and is operated by the national hydrological service DREAL Grand-Est (station code: A1350310, WGS84 coordinates: Lon=7.384773 Lat=48.102498). This station is of interest since it is affected by aquatic seasonal vegetation and has been gauged frequently. A pressure gauge has recorded continuously the stage since 1958. Gaugings were made either with current meters or hydroacoustic profilers (ADCP). Figure 3 gives details about the station location, its surrounding environment and the type of plant present on the site.

Around the station, floodplains are bounded by well-maintained dikes on both sides. A small dam and a weir with a fish-way are present at approximately 800 m upstream of the station and 3.6 km downstream of the station, respectively. The weir is too distant from the station to control the flow. For in-stream flows ($h < 3$ m), a rectangular channel control is assumed. The main channel vegetation influence noticed by the field hydrologists is within this water depth range. No vegetation from the bank blocks the flow. When the flow reaches the floodplains (i.e. water depth above 3 m), the hydraulic control becomes more complex. The flow section changes radically and can be approximated by a combination of the main channel (represented by a wide and rectangular channel) and the two floodplains (represented by a single wide and rectangular channel). In this study, the focus is made only on flows for stages lower than 3 m.

The riverbed at the station is sand-dominated and flat with no large bedforms. In-stream vegetation is composed of flexible and filamentous macrophytes that are, most of the time, just-submerged or not deeply submerged. Plants are mainly Ranunculus. As they grow, they tend to concentrate near the water surface. The height of the deflected vegetation within the channel was never evaluated by the local staff, so no quantitative estimation of the relative submergence range at this station is available. According to the station managers, the plant species has not changed over the years and the riverbed stayed quite stable. The plant density at the station can nevertheless vary from year to year, but no quantitative estimation of these variations was provided by the hydrometric service. The macrophytes always die during winter or are washed out before the end of the year; no dormant vegetation is observed. Conditions are thus appropriate for applying the temporal vegetation model.

4.2 Experimental set-up

4.2.1 Data

Hydraulic gaugings (measurements of h and Q) from January 1996 to August 2017 were performed with a high frequency at the station (generally one gauging every 15 days). A total of 492 measurements of h and Q were carried out under the condition $h < 3$ m. The measurements were sometimes associated with comments about vegetation at the time of gauging. Typical comments were: no plant, few plants, many blooming plants.

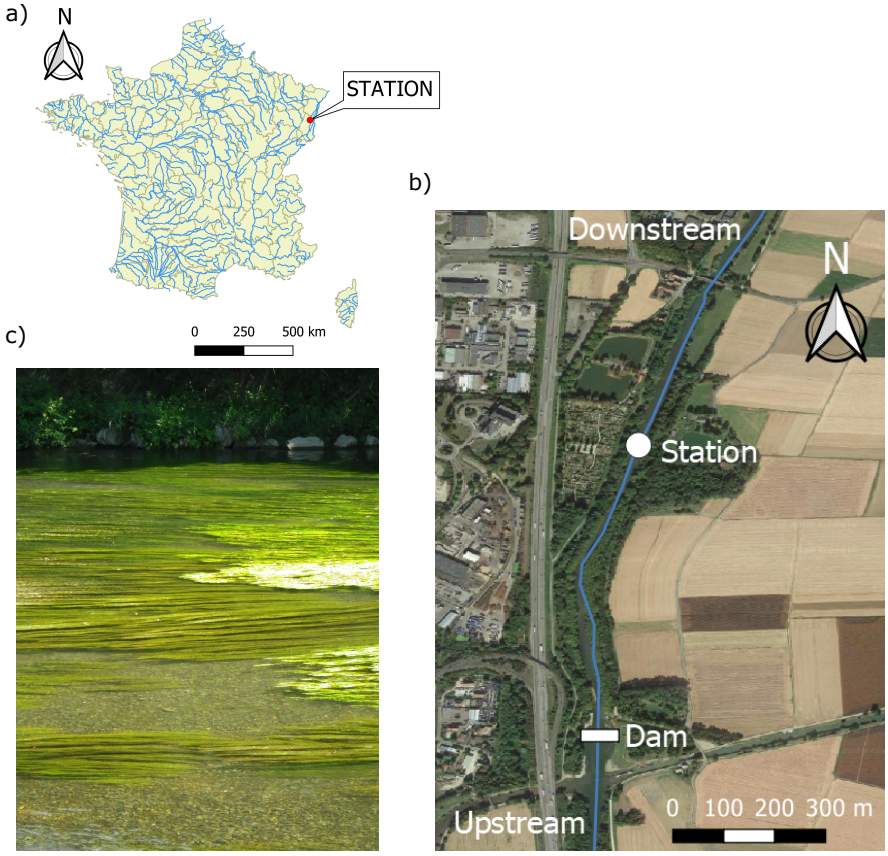

Figure 3: The Ill River at Ladhof hydrometric station: a) its location in France, b) aerial view of its surrounding environment and c) the type of aquatic vegetation (Ranunculus) present in the main channel.

A total of 293 comments are available among the 492 hydraulic gaugings. In the following, they are referred to as vegetation observations. We also have access to additional data such as water level from the French national hydrological database (`http://www.hydro.eaufrance.fr/`), air temperature and irradiance time series from the atmospheric Safran re-analysis over France (Vidal et al., 2010) and data collected from the station managers such as water temperature time series since 2009.

4.2.2 Estimation

Calculations are made over a 22-year data period, where sudden rating curve changes due to morphological evolution happened. The proposed rating curve model accounts for transient changes due to vegetation evolution only (i.e. deviations from the base rating curve due to the presence of plants). Sudden changes due to bed evolution need to be dealt with using another approach (Mansanarez et al., 2019). The vegetation model should be used over stable periods, meaning periods where no significant changes in terms of river geometry are detected, i.e. no variations of S_0, B, n_b, b or c. If the sudden change is not identified before using the vegetation model, interference with the estimation of plant-related parameters could happen, namely with χ, U_χ, d_{max}, t_b, t_m, t_e. The dataset is therefore divided into several stable periods following the method presented in Appendix B. Four stable periods are identified over the 22-year period. Only bed offset b is chang-

ing across these four periods, which reflects bed erosion and deposition at the station; the other parameters S_0, B, n_b, c of the BRC do not change over the entire data-set period.

A 15% uncertainty is set for all the discharge measurements, which is fairly high but reflects the challenging conditions of measurements at this site (low flow velocity and water depth, presence of vegetation, soft surface riverbed). Uncertainty related to the water level measurement is neglected. The vegetation observations transcribed into a position within the plant cycle (see Sections 3.1 and 3.2) are also affected with large uncertainty, since the interpretation of the station manager comments is subjective.

4.2.3 Priors

The prior distributions of the model parameters are given in Table 2. Our knowledge about the plant species at the station and their behaviour is limited, leading to wide priors for parameters related to plant development. The prior distribution for bed slope S_0 was chosen taking into account the difficulty to measure bed slopes in plains. In lowlands, bed slopes are quite low and it is often challenging to identify the right part of the channel for the measurement to have a representative value of the bed slope at the station. The same priors were given for series of parameters that need to be re-estimated for each new stable period (i.e. b) as well as for vegetation parameters that evolve every year (t_b, t_m, t_e and d_{max}). As the plant species was the same over the 22 years of data, parameter χ reflecting the plant flexibility is constant over the entire period. The prior for d_{max} is deliberately imprecise. It was chosen to represent values of d_{max} that can lead to a coefficient of resistance related to plant development, i.e. n_v considering no reconfiguration correction, twelve times higher than the coefficient of resistance related to the bed without vegetation n_b.

5 Results

In this section, the performance of the temporal vegetation model is investigated using the data from Ladhof station. The model is evaluated in terms of parameter identification and relative errors. We also explore the interest of accounting for the plant reconfiguration effect. Using various tests derived from the Ladhof dataset, the importance of using various types of information for estimating the rating curve (i.e. gaugings and vegetation observation) is highlighted.

5.1 Parameters estimation

Figure 4 shows the prior and posterior distributions of the estimated parameters in the form of boxplots. The convergence of MCMC samples is verified visually for all the parameters. Most parameters are well-identified meaning that their posterior distributions are more precise than their prior ones; this is the case for most BRC parameters of each stable periods and for χ (i.e. posterior boxplots are three times narrower for n_b, S_0, χ and up to 16 times narrower for b). Parameters related to plant-development show varying properties depending on the years. Except for a few years (e.g. 2001 and 2017), posterior distributions of t_e are quite precise (14 narrower than prior distribution, on average). For the other three parameters (d_{max}, t_b and t_m), posterior boxplots stay rather wide (between 4 and 6 times narrower than prior boxplots, on average). Data for the year 2017 are only available for half of the year, which might partly explain the poor identification of those plant-development parameters. Their posterior distributions are nevertheless more precise than their prior ones, and would probably be even more precise with additional information.

The parameters describing the timing of the vegetation cycle are always located at approximately the same time over the years (see Figure 4). It is important to recall

Table 2: Prior distributions of the temporal vegetation model parameters for the Ill at Ladhof study case.

Parameter	Distribution
Control channel	
B [m]	$\mathcal{LN}(\ln(25); 0.1)$
S_0 [-]	$\mathcal{LN}(\ln(0.001); 0.5)$
n_b [$\mathrm{m}^{-1/3}$s]	$\mathcal{LN}(\ln(0.02); 0.2)$
b_i [m]	$\mathcal{N}(0.8; 0.2)$
c [-]	$\mathcal{N}(1.67; 0.025)$
Vegetation parameters	
χ [-]	$\mathcal{N}(-1.4; 0.2)$
U_χ [m/s]	$= 0.1$ (fixed)
$t_{b,j}$ [yr]	$\mathcal{U}(0; 1)$
$t_{m,j}$ [yr]	$\mathcal{U}(0; 1)$
$t_{e,j}$ [yr]	$\mathcal{U}(0; 1)$
$d_{max,j}$ [-]	$\mathcal{U}(0; 5)$
Structural uncertainty parameters	
$\gamma_{Q,1}$ [m^3/s]	$\mathcal{LN}(\ln(1); 1)$
$\gamma_{Q,2}$ [-]	$\mathcal{LN}(\ln(0.5); 1)$
γ_{cos} [-]	$\mathcal{U}(0; 1)$
γ_{sin} [-]	$\mathcal{U}(0; 1)$

$1 \leq i \leq 4$ refers to the selected stable period; $1 \leq j \leq 22$ refers to the selected year within the data period; $\mathcal{LN}(m_{log}; s_{log})$ represents a lognormal variable whose logarithm has mean equal to m_{log} and standard deviation equal to s_{log}; $\mathcal{N}(m_g; s_g)$ corresponds to a Gaussian distribution with a mean m_g and a standard deviation s_g; $\mathcal{U}(a_u; b_u)$ corresponds to a uniform distribution defined by its lower (a_u) and upper (b_u) bounds.

that the plant growth in rivers is mostly driven by two key environmental factors, which are the water temperature and the light intensity (Carr et al., 1997). At Ladhof station, these factors evolve similarly over the years of the entire data-set period, which may explain why some plant-development parameters do not strongly vary over the years. As a consequence, some of them could be fixed over the entire 22-year period to simplify the model. This scenario will be investigated in section 5.3. Some exceptions are noticed about the timing of the vegetation cycle in Figure 4, such as a delay at the beginning of growth in 2016 (see t_b) and a late senescence in 2005 (see t_e). During those two years, no specific anomalies in the water temperature or the irradiance time series were noted.

Maximal proxy biomass d_{max} is more variable from year to year than parameters t_b, t_m, t_e. Remember that d_{max} is a key factor in the expression of n_v (see Equation 12). A strong variation in d_{max} thus reflects a strong variation of flow resistance due to plants. In 1998, the posterior distribution for d_{max} is quite close to the prior higher bound (see Figure 4); this bound was set so that $n_v \approx 12 \times n_b$, which is quite strong for the sole influence of in-stream plants but not unrealistic given the values found in the literature; the Manning coefficient n_v can vary from around 0.025 to $0.4\,\mathrm{m}^{-1/3}$s (Chow, 1959; Coon, 1998; Wang & Zhang, 2019). In their review of flow resistance, Fisher & Dawson (2003) categorize Ranunculus among the 'Submerged fine-leaved' vegetation type with reported Mannings n values from 0.01 to more than 0.45 in some cases. The high values of d_{max} reflecting high value of n_v may also include additional effects such as the possible reduction in wetted area due to plants growing from banks, which were assumed negligible in our case.

Correlations between t_b, t_m, t_e and d_{max} were checked for each year. Figure 5 shows an example of the resulting correlation matrix for the year 2004. It looks similar for other years. In general, a strong correlation between t_m and t_e is noticed; for some specific years and to a lesser extent, correlations between t_b and t_m are also noted. We expect to better identify model parameters by reducing the number of parameters varying per year, for example by estimating a single t_m over the entire period of 22 years.

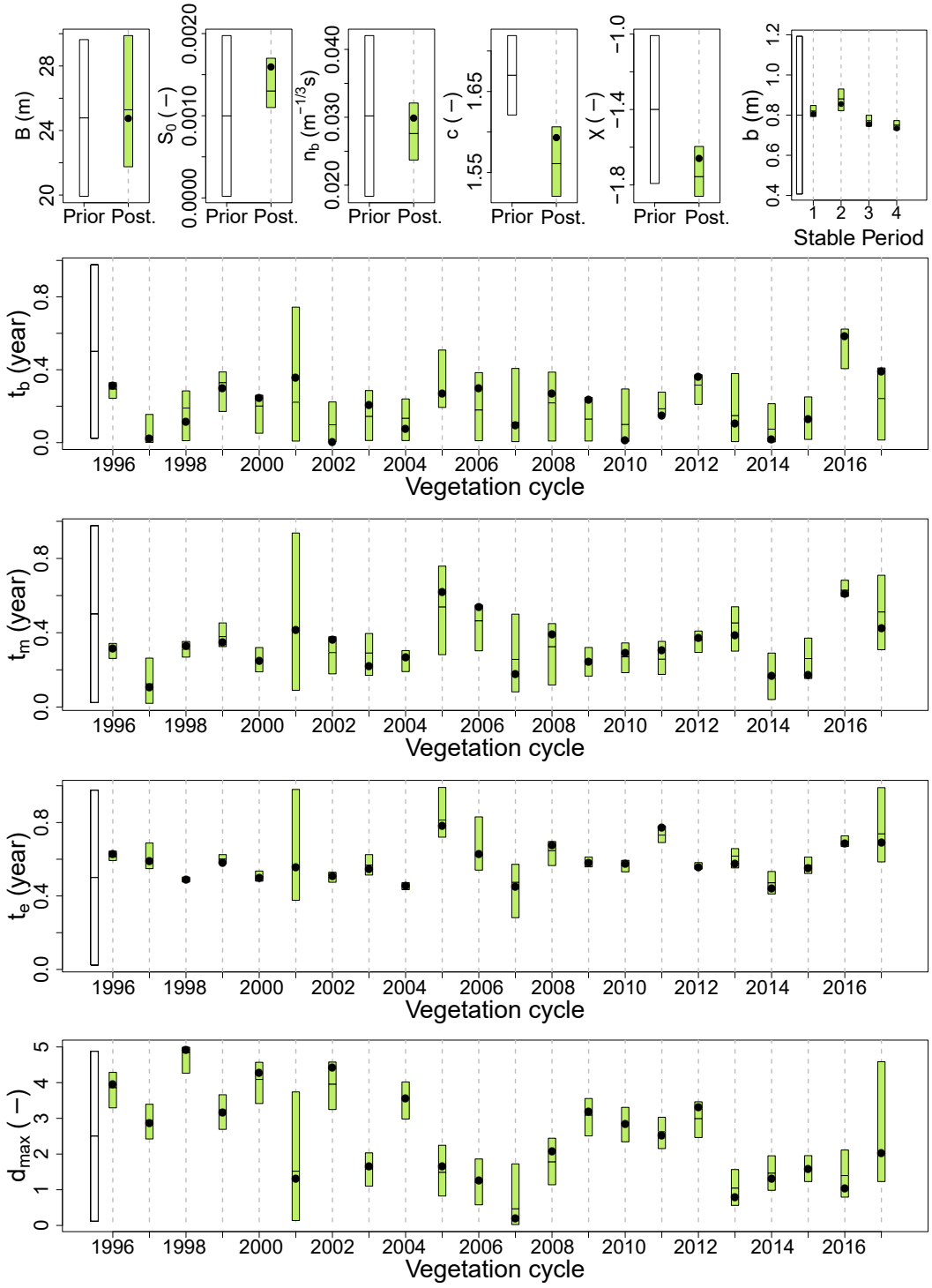

Figure 4: Prior and posterior distributions of the estimated parameters of the vegetation model in case of the Ladhof station over the 22 vegetation years from 1996 to 2017. White and green boxplots relate to the prior and posterior distributions, respectively. The boxes represent the 95% probability interval of the distribution with its median symbolized by a line. Black points refer to parameter values maximising the posterior pdf, also known as maximum a posteriori estimators (MAP).

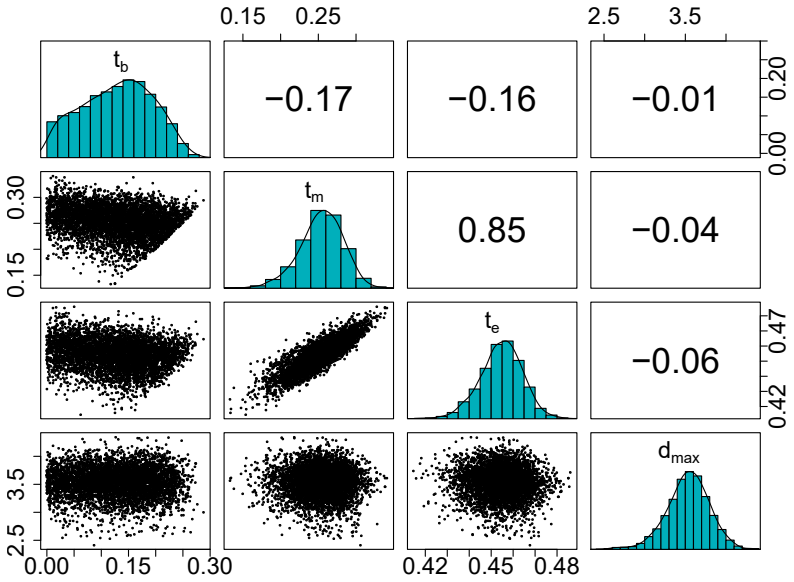

Figure 5: Example of posterior scatterplot correlation matrix between parameters of the plant development model for year 2004.

5.2 Time series reconstruction

Using the stage record at the station and the posterior distributions of the estimated parameters, it is possible to reconstruct the discharge time series $Q(\tau)$ with uncertainty as well as the plant development evolution $d(\tau)$ over the period of 22 years. Figure 6 shows these two time series with uncertainty. The 95% total uncertainty includes both the parametric (i.e. related to estimation errors of the parameters $\boldsymbol{\theta}$ in Equation 18) and structural (i.e. related to structural errors in Equation 20) uncertainties. The "Maxpost" curves correspond to the results obtained using the maximum a posteriori estimates, i.e. parameter-values maximising the posterior pdf. The uncertainty of $Q(\tau)$ is low and the measured and simulated water discharges are close, i.e. within the 20% error range (Figure 6a). For more clarity, a zoom on year 2015 is shown in Figure 6c. The effect of vegetation is generally well-described by the model. For comparison, the computed discharges obtained with a standard model with no vegetation module (see Q_0 in Equation 5) and their associated uncertainty are added to Figure 6c. Total uncertainty is higher when using the model with no vegetation module and observed discharges are better approximated by the vegetation temporal model. The temporal vegetation model is also able to simulate vegetation cycles that are strongly varying from year to year (see $d(\tau)$ in Figure 6b). It is thus possible to account for variable flow resistance induced by the plants. At the Ladhof station, plant cycles have different shapes and amplitudes, which shows that the analysis of the vegetation cycle on a yearly basis is essential even for a case where water temperature and light intensity conditions are similar over the years.

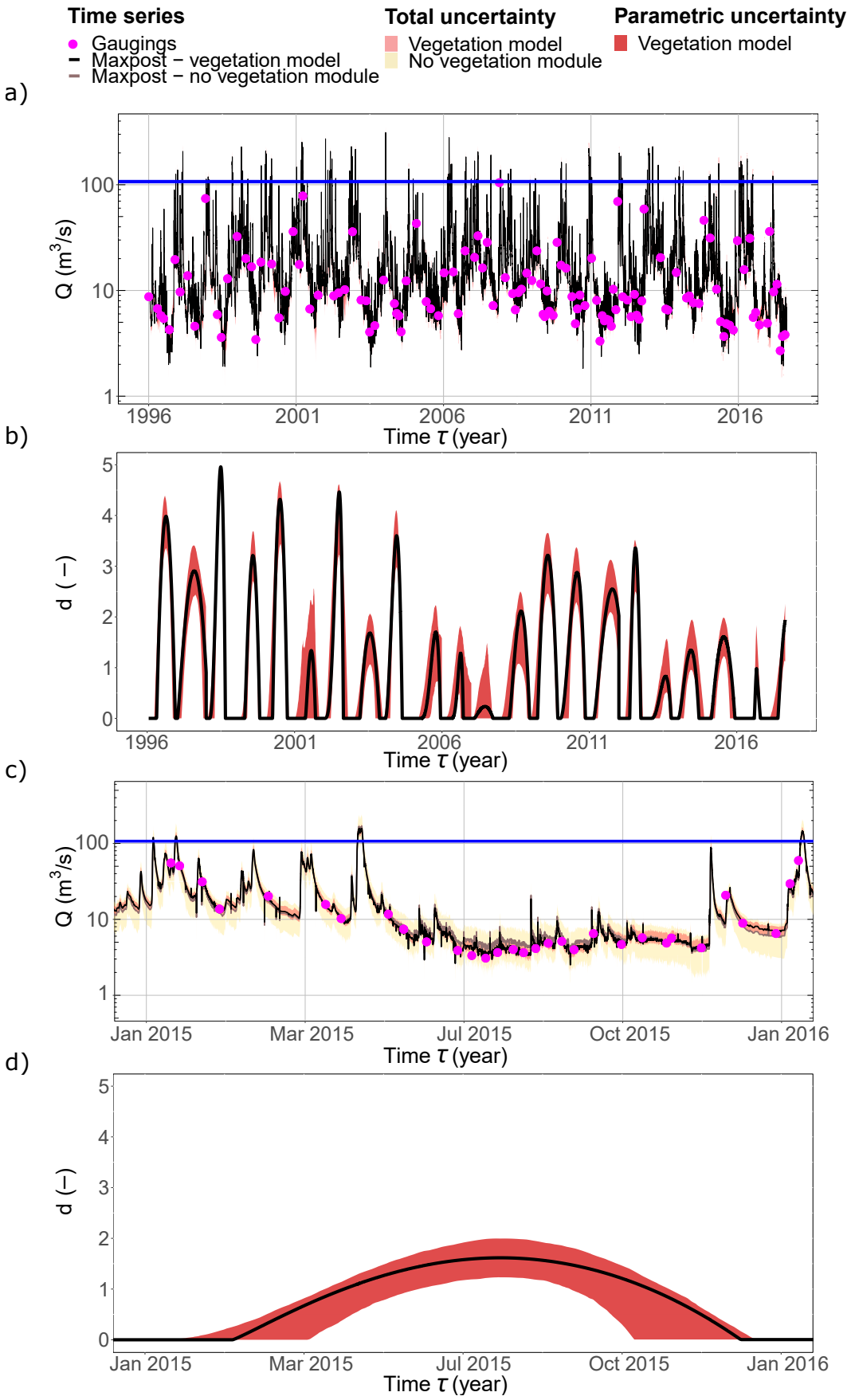

Figure 6: Results obtained with the temporal vegetation model over the 22 years of data at the Ladhof station : a) water discharge time series $Q(\tau)$ with uncertainties, b) time evolution of the plant biomass proxy $d(\tau)$ with parametric uncertainty over the entire period of study, c) water discharge evolution $Q(\tau)$ for year 2015 obtained with the temporal vegetation model and with a standard model with no vegetation module and d) plant evolution $d(\tau)$ for year 2015. Blue lines in b) and c) represent a change in hydraulic control occurring for $h > 3\,\mathrm{m}$: the vegetation model is not valid above this line (see Section 4.1).

5.3 Potential for reducing the number of time-varying parameters

Figure 7 shows the effect of fixing some of the yearly-varying parameters to a constant (but still unknown) value. It compares the relative errors E_r between the gauged discharge and the discharge predicted by the temporal vegetation model (using the MAP estimates).

Relative errors obtained with a standard model with a constant Manning coefficient (no vegetation module) are also added in Figure 7. In that case, E_r can exceed 50% and vary mostly between -28% and +81%. This result highlights the importance of using a rating curve model that accounts for the presence of plants when it is needed through a time-varying Manning coefficient $n_v(t)$. When all parameters related to the plant development vary, E_r values mostly range between ±20%, which is a promising result considering the uncertainty applied to the measured water discharge (15%). Fixing either t_b or t_m does not result in any noticeable increase in relative errors. By contrast, fixing t_e or d_{max} leads to larger relative errors, suggesting that these parameters should be yearly-varying.

For the analyses described in the remainder of the paper, we decided to fix t_m based on the following rationale: a fixed t_m is expected to be very precisely estimated, and this might have the positive side-effect of improving the precision for parameter t_e through the correlation displayed in Figure 5. In these conditions, the model succeeds in identifying parameters and in predicting water discharge with relatively low errors (±20%, see Figure 7).

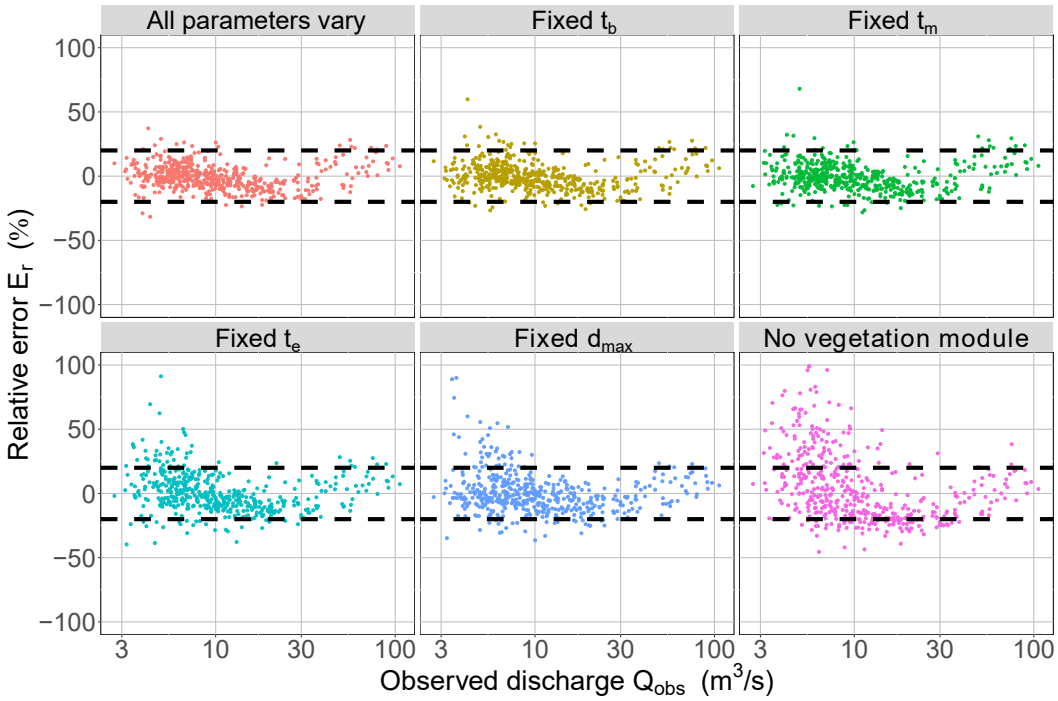

Figure 7: Relative discharge errors E_r for various computation configurations. Dashed lines delimit the ±20% range of errors.

5.4 Reconfiguration versus plant growth

In the rating curve model, it was assumed that the resistance due to aquatic plant was induced by the plant development (growth and decline) but also by the plant ability to reconfigure for high flow velocities. In this section, the relative importance of these two main effects is investigated.

When fixing the reconfiguration coefficient χ to zero, Equation 12 becomes only function of plant development $d(\tau)$. The reconfiguration correction is thus not activated. With $\chi = 0$, plants are assumed to be rigid and not to reconfigure under flow power. To evaluate the importance of the reconfiguration correction in the rating curve model, we compare the discharge obtained with the complete temporal vegetation model accounting for reconfiguration Q_{R} with the discharge obtained with no reconfiguration correction $Q_{\text{no-R}}$. The discharge $Q_{\text{no-R}}$ is computed using the same MAP estimators than those estimated for Q_{R}, except that χ is now fixed to 0 (i.e. the rating curve is not re-estimated). For more details, please refer to Perret et al. (2020).

Figure 8 shows the relative discharge differences due to deactivating the reconfiguration function in the estimated model. Only the data for which vegetation was present were selected and plotted in Figure 8. A large difference in discharge is observed, reaching more than 70%. The reconfiguration correction is larger when the quantity of plant is larger (i.e. $d(\tau)$ is high) and when the mean velocity is higher. The difference between $Q_{\text{no-R}}$ and Q_{R} is negative. Indeed, by contrast to flexible plants, rigid plants cannot bend or align in the flow direction to reduce their frontal areas impacted by the flow. The flow is therefore impeded by their presence. Rigid plants act as strong obstacles. Discharge is thus reduced in presence of rigid plants compared with flexible plants.

In Figure 8, measurements in presence of vegetation and for $U_m \leq 0.3\,\mathrm{m/s}$ are barely available. Nevertheless, it is possible to predict that in this area the difference between $Q_{\text{no-R}}$ and Q_{R} will tend to 0 as we approach the threshold value of $U_m = U_\chi = 0.1\,\mathrm{m/s}$. For reminder, the critical flow velocity for which the plant is able to reconfigure U_χ was fixed to $0.1\,\mathrm{m/s}$ for all the calculations. When $U_m \leq U_\chi$ the plant reconfiguration is made not possible by definition in the model (i.e. the function characterizing the reconfiguration equals the value of 1 in Equation 9). The reconfiguration correction thus becomes inactive.

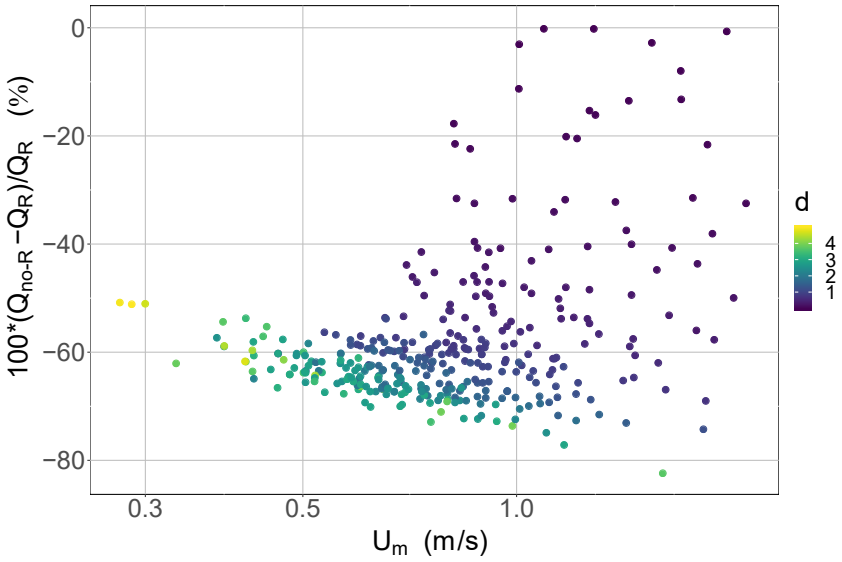

Figure 8: Impact of the reconfiguration correction in the estimated temporal vegetation model versus the gauged mean velocity U_m and the proxy biomass d at the station of the Ill at Ladhof.

5.5 Sensitivity to the number and type of gaugings

At many hydrometric stations, gaugings are less frequent than those perfomed at Ladhof station, and indications about vegetation are generally not available. From the perspective of testing the model in more realistic conditions, the Ladhof station case is subdivided into different tests varying the number and type of available information (i.e. gaugings and vegetation observations) for the computation. These tests are described in Table 3. They were chosen to represent diverse kinds of stations : 1/research stations, where many data are available for estimating the water discharge; the original Ladhof station is considered as a research station; 2/operational stations, more common than research stations and used for surveillance and monitoring purposes; and 3/participatory stations, still rare nowadays, where gaugings are very rare and where most of the vegetation observation comes from the goodwill of outside actors or automatic devices (e.g. photographs of the river section).

The model performance is investigated comparing the test results in terms of parameter identification and relative errors. Figure 9 shows posterior distributions of parameters estimated for all the tests. Figure 10 shows the discharge relative errors obtained with the 283 validation data of tests O1, O2, P1 and P2. For information, discharge relative errors resulting from tests R1 and R2 at the same 283 validation points are added to Figure 10, but note that for these two cases, these points are estimation points too.

The main conclusion arising from these sensitivity tests are summarized in the following:

1. With vegetation information only, estimating time parameters related to plant development is possible (see Figure 9, test P2 and parameters t_b, t_m, t_e). However, for the other parameters the posteriors remain very similar to the priors (see Figure 9, test P2 and parameters d_{max}, B, S_0, n_b, c, χ, b). Unless these priors are very accurate, this procedure leads to fairly large discharge errors (see Figure 10, test P2).

Table 3: Test configurations chosen to evaluate the temporal vegetation model.

		Gaugings			Vegetation observations	
Test	Kind of station	Number of estimation data*	Number of validation data†	Frequency	Number of estimation data*	Frequency
R1	Research	492	0	2/month	293	1/month
R2	Research	492	0	2/month	0	0
O1	Operational	209	283	10/year	119	5/year
O2	Operational	209	283	10/year	0	0
P1	Participatory	88	283	4/year	293	1/month
P2	Participatory	0	283	0	293	1/month

∗: Estimation data are those used for the estimation of the model parameters; they are different from the validation data.
†: Validation data are additional data used only for testing and validating our model; they are the same for tests O1, O2, P1 and P2 in order to compare their results.

2. Adding only a few gaugings per year allows a better estimation of the rating curve parameters (see Figure 9 and compare improvements from tests P2 to P1 for all parameters). While still large, discharge relative error E_r values are already smaller than when using a well-gauged rating curve that ignores vegetation (compare test P1 in Figure 10 versus test with no vegetation module in Figure 7).
3. At the other end of the spectrum, if plenty of gaugings are available and well-distributed over the years, then this suffices to estimate the model (compare test R1 versus test R2 in Figure 9 and 10). A large amount of information is included in the water discharge measurements, including the resistance induced by the vegetation.
4. The operational case is more difficult to interpret as results seem to be parameter-dependent and year-dependent (Figure 9, compare test O1 and test O2). The use of vegetation observations improves the estimation of time parameters for some years but does not have any positive effect on the estimation of the BRC parameters. For the operational cases, most errors are within ±20%, with a few isolated points showing larger errors (Figure 10).

To sum up, the model has a good performance as long as a few gaugings combined with vegetation observations are available. Although vegetation observations are not essential when many gaugings are available, it does help a lot when gaugings are scarce, in particular for the identification of parameters related to plant development.

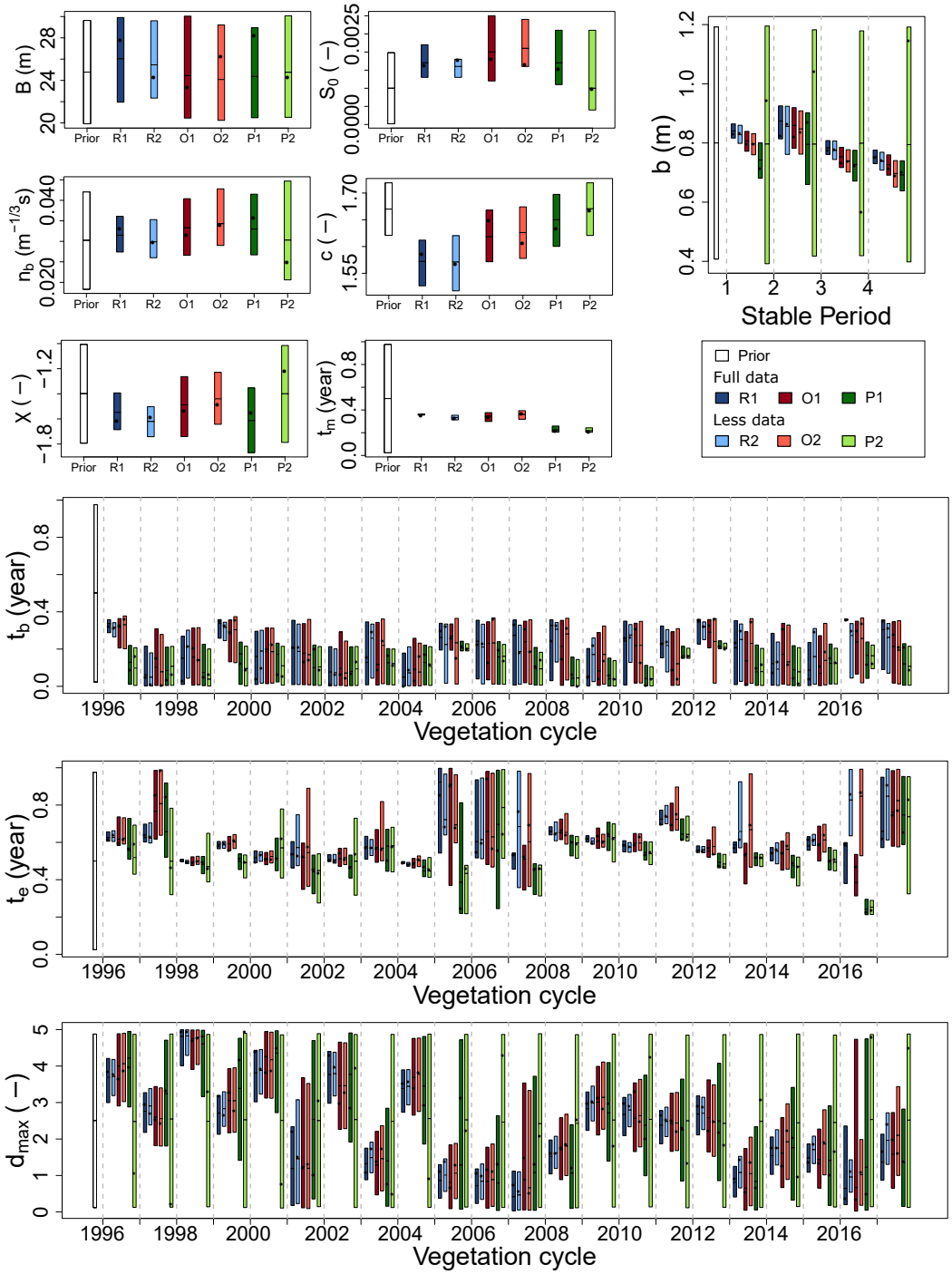

Figure 9: Model sensitivity to the type and number of gaugings or observations. Prior and posterior distributions (95% probability intervals) of the model parameters estimated for all cases presented in Table 3. Black points represent the MAP estimators.

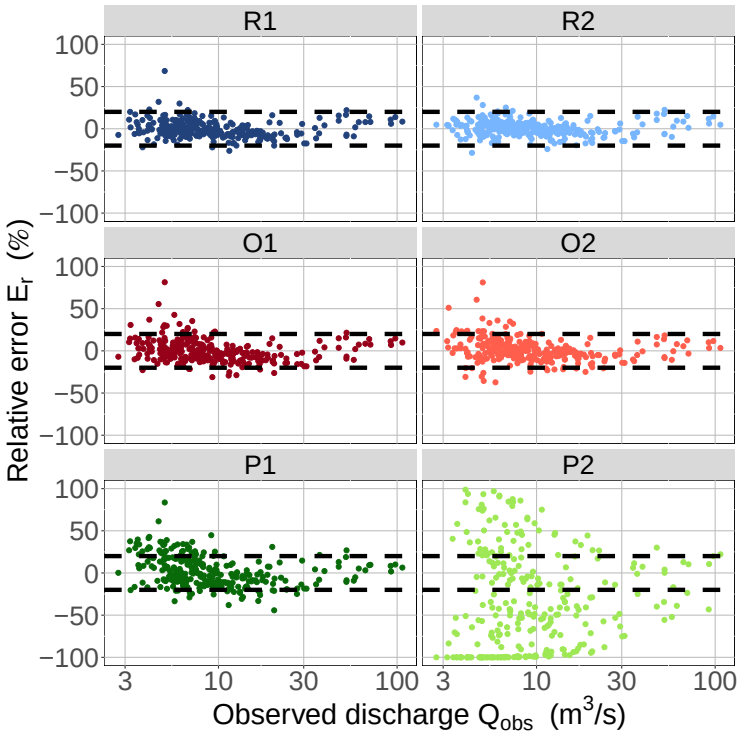

Figure 10: Discharge relative error as a function of observed water discharge obtained for the tests presented in Table 3.

6 Comments on model use and further developments

6.1 How to use the model?

One of the objective of this paper was to develop a rating curve model for operational use. In this part, we detail how the temporal rating curve model can be used in practice. Figure 11 formalizes its functioning. To predict discharge in vegetated flows, an operational user may use the computer implementation of the model that is freely available (see data availability statement). She/he will need to provide the following local information:

1. A data file containing two inputs (i.e. the time and the stage time series recorded at the hydrometric station) and observations (i.e. gaugings and vegetation observations converted into a position into the vegetation cycle using $\cos(\widetilde{\eta}_i)$ and $\sin(\widetilde{\eta}_i)$).
2. Prior specifications for parameters that define the channel control, namely for the channel width B, the channel slope S_0, the base Manning coefficient n_b, and the bed level b.
3. Prior specification for plant-related parameters (i.e. the reconfiguration parameter χ, the reconfiguration velocity U_χ, the characteristic times of the plant cycle (t_b, t_m, t_e) and the maximal proxy biomass d_{max}).

In the model configuration files, non-informative priors can be specified in case no information can be provided a priori. After launching the model runner, the user can have access to the estimated parameters and to four outputs with their parametric and total uncertainty envelopes (see Figure 11), in particular to the discharge $Q(\tau)$ and the proxy biomass $d(\tau)$ time series.

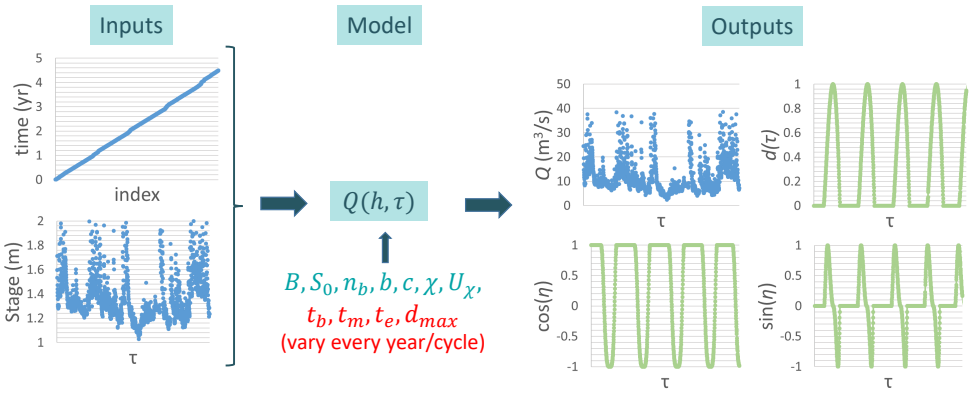

Figure 11: Diagram of the temporal rating curve model for vegetated flows: inputs, parameters and outputs.

6.2 Data collection strategy for vegetation-influenced rating curves

Some suggestions of data collection strategies are made based on our experience of modelling the Ladhof station. The first recommendation is to have information about the aquatic plants present at the station, namely about their nature, morphology and mechanical properties. We therefore advice the station managers to have opinions of experts in aquatic plants in order to improve the estimation of discharge, even if it is not a common practice at hydrometric station. Such information could be used to specify more precise priors for model parameters that are related to plant-development (i.e. t_b, t_m, t_e and d_{max}). Note that even if the plant properties are known specifically, there is

no means to deduce the parameters χ and U_χ precisely. For example, Järvelä (2004) identified the plant species in his study but used laboratory experiments anyway to evaluate empirically these parameters. Look-up tables with χ-values exist for few floodplain plants, but they are still missing for in-stream plants.

Secondly, the distribution of gaugings within the vegetation cycle (i.e. within the year) is likely to be an important factor for a good estimation of the model. Although this point was not explored in the paper, we suggest to have measurements amongst the various states of the vegetation cycle (no plants, growth, peak, decline). In this paper, the gauging measurements were performed about every two weeks and not necessarily scheduled according to the plant cycle.

Finally, this study highlights the importance of having data to characterize the plant development. The plant development is associated to the proxy biomass d in our model, but technically this parameter cannot be measured in the field because it is a proxy. In practice, the angle η is used in the rating curve model to provide information on the state of development of the plant. We thus suggest collecting information describing the position in the plant cycle, which would be used as observational data and would yield valuable information to estimate model parameters. Such information could take the form of simple explicit comments about plant development relative to previous visit at the station, such as *no / same amount of / more / less plants than before*. Comments such as *few plants*, *scarce plants*, *lots of plants*, should be avoided, because they are too vague to be translated into a plant cycle position. Some specific states of the plant cycle are easy to identify such as the vegetation peak, the period without vegetation and the periods of growth and decay. We also recommend collecting quantitative information such as the percentage of channel cross-section covered by vegetation, in order to directly assimilate information about d_0 in the model (i.e. the dimensionless proxy biomass).

As shown in this study, the model can be calibrated using simple observations on the amount of aquatic vegetation that can be made by non biologist observers, e.g. the field hydrologists in charge of streamflow measurement during their field visits. By contrast, post-processing vegetation observation, i.e. transforming them into angles in the development cycle, is generally more time-consuming and complex. For quantifying the plant development cycle, several inexpensive monitoring techniques can be considered such as direct observations (e.g. explicit comments or evaluation of the percentage of channel cross-section covered by vegetation), image analysis from frequent (and automatic) photography of the station or analysing satellite or drone images (Biggs et al., 2018). Indirect vegetation observations could also be deduced from other nearby hydrometric stations, since plant cycles are probably similar as long as the climate and the type of plants are the same at these other stations. Assimilating those data could be a promising development of our model. Thanks to the spatial coherence, these new data would help to better identify the plant parameters of the model and to reduce the uncertainty of the resulting discharge time series at the station.

6.3 Improvements of the rating curve model

The proposed temporal rating curve model is promising for the estimation of water discharge at hydrometric stations affected by aquatic plants. Nevertheless, the discharge relative errors are still high ($-20\,\% < E_r < +20\,\%$) even if acceptable compared with the uncertainty of the gaugings (15 %). In this section, possible improvements of the temporal model proposed in this paper are discussed.

We anticipate that incorporating some biology concepts in the model might lead to better results. Using covariates controlling variations of the plant biomass could help predict the parameters of the vegetation model $d(\tau)$. For example, from their monitoring of the seasonal growth and decay of Ranunculus between 1971 and 1976 in an unshaded section of the River Lambourn at Bagnor, England, Ham et al. (1981) found that

the spatial expansion of Ranunculus in a given year tended to be greater as the mean discharge in spring of that year was greater. Therefore, cumulative discharge in the spring season might be a good candidate for modelling the maximum proxy biomass d_{max} of Ranunculus or similar vegetation. However, Ham et al. (1981) discuss several other influencing factors and mention other sites where high discharge may limit the spatial expansion of Ranunculus. Also, the water temperature (T) or its cumulative form (T_c) could help predict the characteristic times of the plant growth and decay. At hydrometric stations, water temperature is arguably the most common continuously measured parameter after the water level. A possible approach would be to relate t_b to the time where the degree-day had accumulated sufficiently for the plant to start growing ($t_b = t[T_c = T_{c,\min}]$), t_m to the time where the water temperature reaches the optimal temperature T_{opt} for plant growth ($t_m = t[T = T_{\text{opt}}]$), and t_e to the time where the degree-day had accumulated too much, leading to the plant decay ($t_e = t[T_c = T_{c,\max}]$). This method might work for t_b and t_m but less likely for t_e. Indeed, it often happens that the plant decline in natural rivers is driven by plant removal due to high velocities rather than by natural mortality. The optimal temperature T_{opt} and the minimal cumulative degree-day for plant growth $T_{c,\min}$ would be estimated using the Bayesian framework in order to deduce t_b and t_m.

Ultimately, it could be judicious to use a dynamic model rather than a temporal model to predict the plant evolution at hydrometric stations. The evolution of the biomass proxy $d(\tau)$ is cyclic in our model. However, it does not always follow a bell-shaped curve in practice. Plant development can be sometimes subject to perturbations depending on external factors. For example, a brutal variation in water temperature, change in nutrient loads, human plant removal, or a large flood can strongly impact the typical evolution of the plant. A dynamic model that would update the biomass as a function of such external drivers could increase the performance of the rating curve model. Compartment models are often used to describe dynamic behaviour, e.g. reservoir models in hydrology or crop growth compartment models in biology (Johnson & Thornley, 1983). By analogy, the proxy of biomass $d(\tau)$ in rivers could be seen as a stock of biomass that evolves in time according to diverse external factors (Fovet et al., 2010). The production of biomass would be regulated by environmental factors that favor or limit the plant growth, such as the water temperature, the light intensity, the amount of nutrients, etc. The loss of biomass would be modelled by detachments of biomass (due to hydraulic variations, natural senescence, external interventions, etc.). Using such model is promising for the future because these external factors are expected to change according to climate projections (e.g. increase in water temperature, eutrophication). One of the main advantages of using this dynamic approach is that parameters would be estimated one time only for the entire data period and not every year as for the cyclic approach. In addition, more complex stations than Ladhof station could also be dealt with such a dynamic model, such as, for example, stations where plants do not die at the end of each year.

6.4 Extension of the rating curve model to fully submerged or emergent plants

The applicability of the model is limited to specific conditions detailed in Section 2.1. It could be extended by revising those conditions. However, limiting the model complexity is important to ensure that it is applicable for operational purposes.

Importantly, the model applicability is limited to a specific range of relative submergence (close to 1), namely for just-submerged or not deeply submerged plants. To cover as many cases as possible, the model could be extended to emergent and fully submerged plants (i.e. $[h-b]/H_p \leq 1$ and $[h-b]/H_p > 1$, respectively). This would require modifying the flow resistance equation $n_v(\tau)$. Major changes in Equation 9 would be related to the plant density parametrization (because emergent and submerged plants do

not have the same properties) and to the chosen characteristic velocity (because flow structure strongly changes from submerged to emergent plants).

In the case of submerged plants, the flow structure over the section would change and the water volume located above the ground-plants should be accounted for. The flow structure would be composed of two separate vertical layers: one for vegetation and one for overflow. The mean velocity within the vegetated part of the cross-section U_v should be retained as the new characteristic velocity for the computation of n_v, in replacement of the depth-averaged velocity U_m used in our study. The velocity U_v is harder to estimate than U_m, but methods such as the common two-layer approach exist (Luhar & Nepf, 2013; Västilä et al., 2016). The velocity U_v depends on the length of the submerged plants, and hence on their evolution. Using U_v instead of U_m in Equation 9 will thus complicate the flow resistance model, because (i) another proxy for plant development would be needed and (ii) U_m would no longer be the characteristic velocity and its simple relation with the total discharge Q (i.e. $U_m = Q/(B[h-b])$) would not hold anymore.

For emergent plants, no change of parametrization for the characteristic velocity U_c would be needed in the flow resistance equation (i.e. $U_c = U_m$). Indeed, the flow structure would still be composed of one layer. However, the plant density parameter (i.e. $d(\tau)$, which simulates the proxy biomass of the entire vegetation) should be revisited since only the submerged part of the plants needs to be accounted for. Järvelä (2004) suggests that partially submerged plants generally have uniform distributions of LAI over their height, and so adds the relative submergence $[h-b]/H_p$ as a correction in Equation 6. The same type of correction could be applied to Equation 9. It would imply the addition of another time-varying model $H_p(\tau)$ to be able to predict the plant height evolution in function of time.

In our opinion, extending the model to submerged plants should have priority because emergent plants are not often observed in main channels and are more relevant for the study of floodplain flows.

7 Conclusion

This study is a first attempt at deriving a rating curve model for channel controls to predict water discharge time series at hydrometric stations affected by seasonal instream plants. A temporal rating curve model is developed based on the assumption that vegetation induces a change in bed roughness mainly, which modifies the flow resistance. In the model, the bed roughness is described using a time-varying resistance coefficient, which combines the change in resistance due to plant growth and decay, and to the plant ability to reconfigure with high flow velocity (i.e. streamlining and bending). A Bayesian approach using prior knowledge on hydraulic controls at the station and observation data (gaugings and comments about the amount of vegetation) is used for estimating the model parameters and uncertainty. With such an approach, it is possible to compute the water discharge time series over a given time-period along with the evolution of the proxy biomass, which informs about the plant resistance potential.

Several tests are conducted to investigate the model performance using data from a station affected by aquatic vegetation. The relative discharge errors and the parameter identification are analysed and discussed. The relative importance of the two main effects that drive the time-varying resistance coefficient is investigated. Although plant development is the main cause of flow resistance variation, the reconfiguration correction was found to be crucial for the discharge calculation. This correction is especially important when the mean velocity and the plant biomass are large. The tests also suggest that the complexity of the model can be reduced by fixing some year-to-year varying parameters related to plant growth and decay, without reducing the model performance. Both gaugings and vegetation observations are valuable for a good calibration

of the model. Simple comments on the amount of aquatic vegetation yield valuable information for the estimation of the parameters related to the plant growth and decay, especially when hydraulic gaugings are scarce. Finally, the temporal rating curve model accounting for aquatic vegetation can reduce the relative discharge errors to acceptable levels, from a range of $\pm 50\,\%$ to $\pm 20\,\%$ as found in the application case.

Obviously, further tests and the development of guidelines and procedures are needed to prepare the transfer of the proposed method to hydrological services. The main perspectives for model development are the extension to fully submerged plants and the implementation of a dynamic model instead of the temporal approach based on a parameterized shape of the growth and decay cycle from year to year. A dynamic model would predict the biomass evolution based on external and environmental factors that enhance or limit the plant growth. Such an approach will certainly require a deeper knowledge of the plant species, distribution and dynamics at a given site. But again, a trade-off between model complexity and performance should be sought to ensure its operational applicability by field hydrologists.

Appendix A Temporal plant development model

The biomass model is obtained by integrating in time the growth rate model of Yin et al. (2003) (Equation 10):

$$w(t) = \int \frac{dw}{dt} dt = \int GR_{max} \left(\frac{t_e - t}{t_e - t_m} \right) \left(\frac{t - t_b}{t_m - t_b} \right)^p dt \tag{A1}$$

with $p = (t_m - t_b)/(t_e - t_m)$, dw/dt the growth rate, $w(t)$ the biomass, t_b the time at which the plant starts to grow, t_m the time at which the growth rate is the greatest, t_e the end of the growth time and GR_{max} the maximal growth rate.

In the following, the integration of Yin et al. (2003) model is detailed step by step:

$$\int \frac{dw}{dt} dt = \frac{GR_{max}}{t_e - t_m} \left[\int t_e \left(\frac{t - t_b}{t_m - t_b} \right)^p dt - \int t \left(\frac{t - t_b}{t_m - t_b} \right)^p dt \right] \tag{A2}$$

The second part of Equation A2 can be easily integrated by using the equality $t = t - t_b + t_b$:

$$\begin{aligned} \frac{1}{(t_m - t_b)^p} \int t(t - t_b)^p dt =& \frac{1}{(t_m - t_b)^p} \int (t - t_b + t_b)(t - t_b)^p dt \\ =& \frac{1}{(t_m - t_b)^p} \left(\int (t - t_b)(t - t_b)^p dt + \int t_b (t - t_b)^p dt \right) \\ =& \frac{1}{(t_m - t_b)^p} \left[\frac{(t - t_b)^{p+2}}{p+2} + t_b \frac{(t - t_b)^{p+1}}{p+1} \right] \\ =& \frac{1}{(t_m - t_b)^p} (t - t_b)^{p+1} \frac{pt + t + t_b}{(p+2)(p+1)} + C_0 \end{aligned} \tag{A3}$$

with C_0 a constant equal to zero since $w(t = t_b) = 0$.

Going back to the integration of the entire model, Equation A2 becomes:

$$\begin{aligned} w(t) =& \frac{GR_{max}}{t_e - t_m} \left[t_e \left(\frac{t - t_b}{t_m - t_b} \right)^p \frac{(t - t_b)}{(p+1)} - \frac{(t - t_b)^{p+1}}{(t_m - t_b)^p} \frac{(pt + t + t_b)}{(p+2)(p+1)} \right] \\ =& \frac{GR_{max}}{t_e - t_m} \left(\frac{t - t_b}{t_m - t_b} \right)^p (t - t_b) \left[\frac{(p+2)t_e - (p+1)t - t_b}{(p+2)(p+1)} \right] \end{aligned} \tag{A4}$$

We now assume that the maximum of biomass w_{max} is reached at $t = t_e$. To calculate w_{max}, t is replaced by t_e in Equation A4:

$$w_{max} = \frac{GR_{max}}{t_e - t_m} \left(\frac{t_e - t_b}{t_m - t_b} \right)^p (t_e - t_b) \left[\frac{t_e - t_b}{(p+2)(p+1)} \right] \tag{A5}$$

The biomass model is deduced from the comparison between Equations A4 and A5, by forming the ratio $w(t)/w_{max}$:

$$\begin{aligned}\frac{w(t)}{w_{max}} &= \left(\frac{t-t_b}{t_e-t_b}\right)^p \frac{(t-t_b)}{(t_e-t_b)}\left[\frac{(p+2)t_e-(p+1)t-t_b}{t_e-t_b}\right] \\ &= \left(\frac{t-t_b}{t_e-t_b}\right)^{p+1}\left[\frac{(p+2)t_e-(p+1)t-t_b}{t_e-t_b}\right]\end{aligned} \tag{A6}$$

Reminding that $p=(t_m-t_b)/(t_e-t_m)$, the final biomass model can be expressed as follows:

$$w(t) = w_{max}\left(\frac{t-t_b}{t_e-t_b}\right)^{\frac{t_e-t_b}{t_e-t_m}}\left[\frac{2t_e-t_m-t}{t_e-t_m}\right] \tag{A7}$$

Appendix B Identification of stable periods

This appendix details the method used for identifying stable periods where no significant changes in terms of river geometry can be detected. Over a stable period, no sudden changes (due to bed evolution) in the rating curve should be observed.

We assume that significant change in riverbed happens after a morphogenic flood (Mansanarez et al., 2019). The date following the flood event marks the beginning of a new stable period. For convenience, morphogenic flood is arbitrarily defined as a flood exceeding the 2-year flood ($Q > Q_2$). For the Ladhof station, the possible changes after such a flood are overall bed erosion or deposition at the station according to station managers. In other words, it might induce a change in the offset of the main channel control b. No particular variations of channel slope S_0, channel width B and bed roughness n_b have been previously noticed over the years. Note that at the Ladhof station, the vegetation disappears every winter and n_b depends on the type of sediments and bedforms present on the riverbed only. Consequently, only one parameter of the BRC needs to be re-estimated when a new stable period begins. Ten stable periods were identified based on $Q > Q_2$ for the Ladhof station over the 22 years of data. The stage time series (Figure B1a) show that even after floods the riverbed level does not obviously vary. The number of stable periods can thus be further reduced.

Base rating curves of the ten periods were estimated using the classical power-law model and the Bayesian method presented in Le Coz et al. (2014):

$$\begin{cases} Q(h,\tau) = \dfrac{1}{n_b} B\sqrt{S_0}[h(\tau)-b]^c \text{ for } h > b \\ Q(h,\tau) = 0 \text{ for } h \leq b \end{cases} \tag{B1}$$

The base rating curves are shown in Figure B1b along with the posterior distributions of b in Figure B1c. The estimation of b is sometimes uncertain due to the small number of gaugings available over the considered periods (see gaugings from period 1 for example). Combining visual observations of the BRC (Figure B1b) and analysis of the riverbed level evolution (Figure B1c), the 22 years of data were divided into four periods. If two successive BRCs overlap and if the posterior distribution of b is in the same range, we assume that no changes have happened and that the two successive periods can be merged. The initial 10 stable periods are hence merged into four stable periods with this comparison technique. Figure B1d and Figure B1e show the characteristics of the BRCs for the new four periods.

Acknowledgments

This work was funded by SCHAPI, France's national hydrological service (SRNH 2018 and 2019 contracts between INRAE and the Ministry of Ecology). Data for the Ladhof

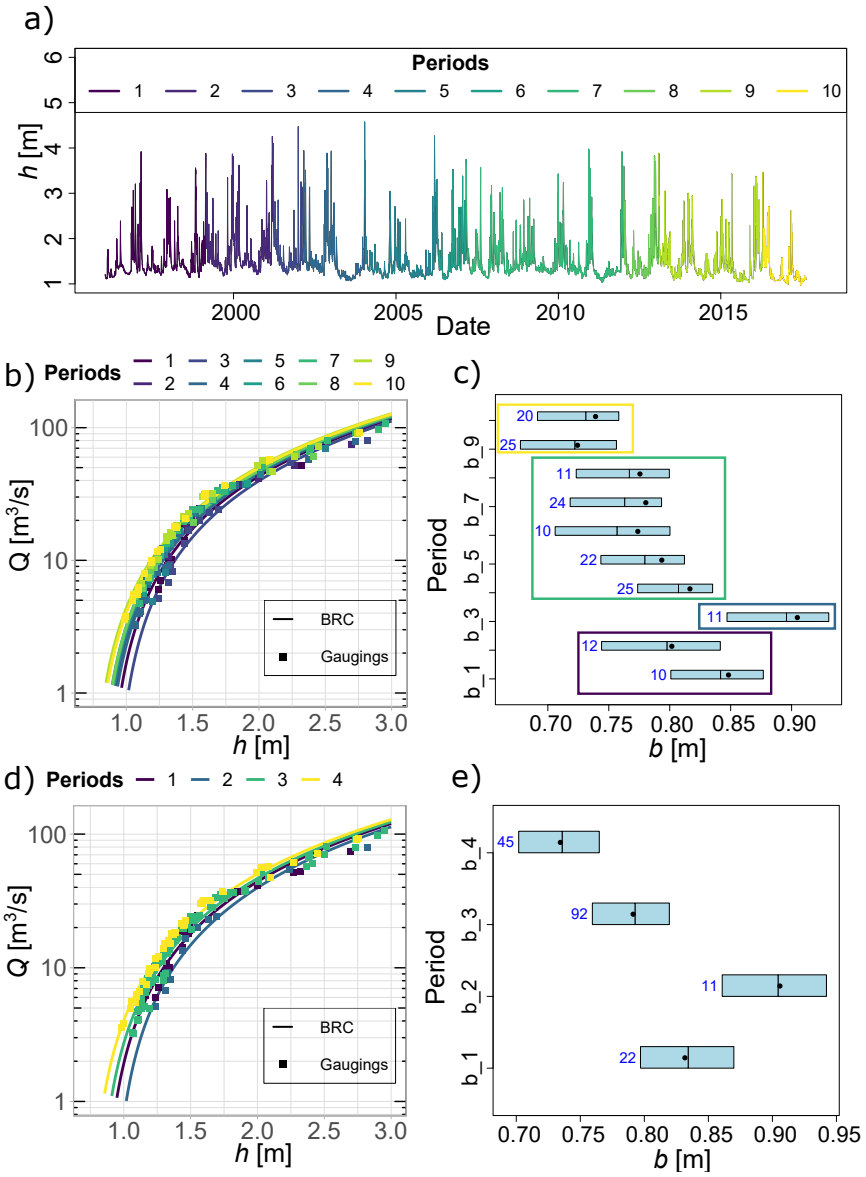

Figure B1: Identification of stable periods at the Ill at Ladhof hydrometric station over the 22-year of data available: a) stage time series of the ten periods defined by $Q > Q_2$ flood events, b) base rating curves (BRC) estimated using Bayesian method for the ten periods and c) distributions of the riverbed level b, and d) BRC estimated using Bayesian method for the four resulting periods and e) distributions of b. Blue numbers refer to the number of gaugings without vegetation used for computing the BRC over the considered period. Colored rectangles in b) highlight the four final periods.

station were provided by the DREAL Alsace/Grand-Est. Data were mostly collected by Daniel Moritz and his colleague Vincent Mossard. We gratefully thank them for their contribution. The authors would also like to thank Juha Järvelä, Sara Puijalon and Ellis Penning for the interesting discussions we had in the earlier stages of this work. We finally want to thank the two anonymous reviewers and Paul A. Carling, associate editor and editor for their valuable and insightful comments, which have undoubtedly improved this paper.

Competing interests. The authors declare that they have no conflict of interest.

Data availability statement The data set and the data processing algorithms used in this study are available on request from the authors and are archived in `https://forge.irstea.fr/projects/bam/files` (folder name: Perret_VegetationPaper_WRR.zip)..

References

Aberle, J., & Järvelä, J. (2013). Flow resistance of emergent rigid and flexible floodplain vegetation. *Journal of Hydraulic Research*, *51*(1), 33-45.

Adams, M.-P., Collier, C., Uthicke, S., Ow, Y.-X., Langlois, L., & O'Brien., K. (2017). Model fit versus biological relevance: Evaluating photosynthesis-temperature models for three tropical seagrass species. *Scientific reports*, *7*(39930), 1-12. doi: 10.1038/srep39930

Albayrak, I., Nikora, V., Miler, O., & O Hare, M. (2014). Flow-plant interactions at leaf, stem and shoot scales: drag, turbulence, and biomechanics. *Aquatic Sciences*, *76*(2), 269-294. doi: 10.1007/s00027-013-0335-2

Arcement, G.-J., & Schneider, V.-R. (1989). Guide for selecting Manning's roughness coefficients for natural channels and flood plains. *U.S. Geological Survey Water Supply*, *Paper 2339*, 1-67.

Asaeda, T., Trung, V., Manatunge, J., & Bon, T. (2001). Modelling macrophyte - nutrient - phytoplankton interactions in shallow eutrophic lakes and the evaluation of environmental impacts. *Ecological Engineering*, *16*, 341-357.

Barnes, H.-H. (1967). Roughness characteristics of natural channels: color photographs and descriptive data for 50 stream channels for which roughness coefficients have been determined. *U.S. Geological Survey Water Supply*, *Paper 1849*.

Biggs, H., Nikora, V., Gibbins, C., Fraser, S., Green, D., Papadopoulos, K., & Hicks, D. (2018). Coupling Unmanned Aerial Vehicle (UAV) and hydraulic surveys to study the geometry and spatial distribution of aquatic macrophytes. *Journal of Ecohydraulics*, *3*(1), 45-58. doi: 10.1080/24705357.2018.1466666

Briére, J.-F., Pracros, P., Roux, A.-Y.-L., & Pierre, J. (1999). A novel rate model of temperature-dependent development for arthropods. *Environmental Entomology*, *28*, 22-29.

Carr, G.-M., Duthie, H.-C., & Taylor, W. (1997). Models of aquatic plant productivity: a review of the factors that influence growth. *Aquatic Botany*, *59*, 195-215.

Chow, V.-T. (1959). *Open-channel hydraulics*. McGraw-Hill, NewYork.

Coelho, D.-T., & Dale, R.-F. (1980). An energy-crop growth variable and temperature function for predicting maize growth and development: planting to silking. *Agronomy journal*, *72*, 503-510.

Coon, W. (1998). Estimation of roughness coefficients for natural stream channels with vegetated banks. *U.S. Geological Survey Water Supply*, *Paper 244*, 145.

Cowan, W.-L. (1956). Estimating hydraulic roughness coefficients. *Agricultural Engineering*, *37*(7), 473-475.

de Langre, E. (2008). Effect of wind on plants. *Annual Review of Fluid Mechanics*, *40*, 141-168. doi: 10.1146/annurev.fluid.40.111406.102135

Fathi-Maghadam, M., & Kouwen, N. (1997). Nonrigid, nonsubmerged, vegetative roughness on floodplains. *Journal of Hydraulic Engineering*, *123*(1), 51-57. doi: doi:10.1061/(ASCE)0733-9429(1997)123:1(51)

Fisher, K., & Dawson, F. H. (2003). *Reducing uncertainty in river flood conveyance - Roughness review* (Tech. Rep.). London, UK: DEFRA / Environment Agency, Project W5A-057.

Folkard, A.-M. (2011). Vegetated flows in their environmental context: a review. *Proceedings of the Institution of Civil Engineers - Engineering and Computational*

Mechanics, *164*(1), 3-24.

Fovet, O., Belaud, G., Litrico, X., Charpentier, S., Bertrand, C., Dauta, A., & Hugodot, C. (2010). Modelling periphyton in irrigation canals. *Ecological Modelling*, *221*, 1153-1161. doi: 10.1016/j.ecolmodel.2010.01.002

Green, J. (2005). Comparison of blockage factors in modelling the resistance of channels containing submerged macrophytes. *Rivers Research and Applications*, *21*, 671-686. doi: 10.1002/rra.854

Ham, S. F., Wright, J. F., & Berrie, A. D. (1981). Growth and recession of aquatic macrophytes on an unshaded section of the River Lambourn, England, from 1971 to 1976. *Freshwater Biology*, *11*, 381-390.

Hicks, D.-M., & Mason, P.-D. (1999). *Roughness characteristics of New Zealand rivers*. NIWA, Christchurch.

Hilton, J., O'Hare, M., Bowes, M., & Jones, J. (2006). How green is my river? a new paradigm of eutrophication in rivers. *Science of the Total Environment*, *365*, 66-83.

Horner, I., Renard, B., Le Coz, J., Branger, F., McMillan, H. K., & Pierrefeu, G. (2018). Impact of stage measurement errors on streamflow uncertainty. *Water Resources Research*, *54*(1952-1976).

Jalonen, J. (2015). *Hydraulics of vegetated flows: estimating riparian plant drag with a view on laser scanning applications* (PhD Thesis). Aalto University School of Engineering.

Järvelä, J. (2004). Determination of flow resistance caused by non-submerged woody vegetation. *International Journal of River Basin Management*, *2*(1), 61-70. doi: 10.1080/15715124.2004.9635222

Johnson, I., & Thornley, J. (1983). Vegetative crop growth model incorporating leaf area expansion and senescence, and applied to grass. *Plant, Cell and Environment*, *6*, 721-729.

Kiang, J., Gazoorian, C., McMillan, H., Coxon, G., Le Coz, J., & Westerberg, I. (2018). A comparison of methods for streamflow uncertainty estimation. *Water Resources Research*, *54*, 7149-7176. doi: https://doi.org/10.1029/2018WR022708

Kouwen, N., & Fathi-Moghadam, M. (2000). Friction factors for coniferous trees alons rivers. *Journal of Hydraulic Engineering*, *126*(10), 732-740.

Le Coz, J., Renard, B., Bonnifait, L., Branger, F., & Le Boursicaud, R. (2014). Combining hydraulic knowledge and uncertain gaugings in the estimation of hydrometric rating curves: A Bayesian approach. *Journal of Hydrology*, *509*, 573-587. doi: https://doi.org/10.1016/j.jhydrol.2013.11.016

Limerinos, J.-T. (1970). Determination of the Manning coefficient from measured bed roughness in natural channels. *U.S. Geological Survey Water Supply*, *Paper 1898-B*.

Luhar, M., & Nepf, H. (2013). From the blade scale to the reach scale: a characterization of aquatic vegetative drag. *Advances in Water Resources*, *51*, 305-316. doi: 10.1016/j.advwatres.2012.02.002

Lundquist, J. D., Roche, J. W., Forrester, H., Moore, C., Keenan, E., Perry, G., ... Dettinger, M. D. (2016). Yosemite hydroclimate network: Distributed stream and atmospheric data for the tuolumne river watershed and surroundings. *Water Resources Research*, *52*, 7478-7489.

Mansanarez, V. (2016). *Non-unique stage-discharge relations: Bayesian analysis of complex rating curves and their uncertainties* (PhD Thesis). Université Grenoble Alpes.

Mansanarez, V., Renard, B., Le Coz, J., Lang, M., & Darienzo, M. (2019). Shift happens! adjusting stage-discharge rating curves to morphological changes at known times. *Water Resources Research*, *55*, 2876-2899. doi: https://doi.org/10.1029/2018WR023389

McMillan, H., Seibert, J., Petersen-Overleir, A., Lang, M., White, P., & Snelder, T.

(2017). How uncertainty analysis of streamflow data can reduce costs and promote robust decisions in water management applications. *Water Resources Research*, *53*, 5220-5228. doi: https://doi.org/10.1002/2016WR020328

Meyer-Peter, E., & Müller, R. (1948). Formulas for bed-load transport. In *Proceedings of the 2nd iahr congress* (p. 39-64). Stockholm, Sweden.

Morin, J., Leclerc, M., Secretan, Y., & Boudreau, P. (2000). Integrated two-dimensional macrophytes-hydrodynamic modeling. *Journal of Hydraulic Research*, *38*(3), 163-172. doi: doi:10.1080/00221680009498334

Neary, V., Constantinescu, S., Bennett, S., & Diplas, P. (2012). Effects of vegetation on turbulence, sediment transport, and stream morphology. *Journal of Hydraulic Engineering*, *138*(9), 765-776.

Nepf, H.-M. (2012). Hydrodynamics of vegetated channels. *Journal of Hydraulic Research*, *50*(3), 262-279.

Nikora, V. (2010). Hydrodynamics of aquatic ecosystems: An interface between ecology, biomechanics and environmental fluid mechanics. *River Research and Applications*, *26*, 367-384. doi: https://doi.org/10.1002/rra.1291

Olsen, J., McMahon, C.-R., & Hammer, G.-L. (1993). Prediction of sweet maize phenology in subtropical environments. *Agronomy journal*, *85*, 410-415.

Pasche, E., & Rouvé, G. (1985). Overbank flow with vegetatively roughened flood plains. *Journal of Hydraulic Engineering*, *111*(9), 1262-1278.

Perret, E., Le Coz, J., & Renard, B. (2020). Estimating time-varying stage-discharge relations in rivers with aquatic vegetation. In *10th Conference on Fluvial Hydraulics, IAHR-River Flow.* Delft, The Netherland.

Petryk, S., & Bosmajian, G. (1975). Analysis of flow through vegetation. *Journal of Hydraulic Division*, *101*(7), 871-884.

Rantz, S. E. (1982). *Measurement and computation of streamflow : Volume 1. Measurement of stage and discharge.* (Tech. Rep.). USGS.

Rantz, S. E. (1982). *Measurement and computation of streamflow: Volume 2. Computation of discharge.* (Tech. Rep.). USGS.

Renard, B., Garreta, V., & Lang, M. (2006). An application of Bayesian analysis and Markov Chain Monte Carlo methods to the estimation of a regional trend in annual maxima. *Water Resources Research*, *42*(W12422). doi: http://dx.doi.org/10.1029/2005WR004591?

Room, P.-M. (1986). Equations relating growth and uptake of nitrogen by salvinia molesta to temperature and the availability of nitrogen. *Aquatic Botany*, *24*, 43-59.

Shields, F.-D., Coulton, K., & Nepf, H. (2017). Representation of vegetation in two-dimensional hydrodynamic models. *Journal of Hydraulic Engineering*, *143*(8), 1-9. doi: 10.1061/(ASCE)HY.1943-7900.0001320

Smart, G. M., Maurice, M. J., & Walsh, J. M. (2002). Relatively rough flow resistance equations. *Journal of Hydraulic Engineering*, *128*(6), 568-578.

Tollenaar, M., Daynard, T.-B., & Hunter, R.-B. (1979). Effect of temperature on rate of leaf appearance and flowering date in maize. *Crop Science*, *19*, 363-366.

van der Heide, T., Roijackers, R.-M.-M., van Nes, E.-H., & Peeters, E.-T.-H.-M.-. (2006). A simple equation for describing the temperature dependent growth of free-floating macrophytes. *Aquatic Botany*, *84*, 171-175.

Vargas-Luna, A., Crosato, A., & Uijttewaal, W. (2015). Effects of vegetation on flow and sediment transport: comparative analyses and validation of predicting models. *Earth Surface Processes and Landforms*, *40*, 157-176. doi: 10.1002/esp.3633

Västilä, K., & Järvelä, J. (2014). Modeling the flow resistance of woody vegetation using physically based properties of the foliage and stem. *Water Resources Research*, *50*, 229-245. doi: 10.1002/2013WR013819

Västilä, K., & Järvelä, J. (2017). Characterizing natural riparian vegetation for modeling of flow and suspended sediment transport. *Journal of Soils and Sedi-*

ments, 1-17. doi: 10.1007/s11368-017-1776-3

Västilä, K., Järvelä, J., & Aberle, J. (2013). Characteristic reference areas for estimating flow resistance of natural foliated vegetation. *Journal of Hydrology*, *492*, 49-60. doi: http://dx.doi.org/10.1016/j.jhydrol.2013.04.015

Västilä, K., Järvelä, J., & Koivusalo, H. (2016). Flow-vegetation-sediment interaction in a cohesive compound channel. *Journal of hydraulic Engineering*, *142*(1).

Vidal, J.-P., Martin, E., Franchistéguy, L., Baillon, M., & Soubeyroux, J.-M. (2010). A 50-year high-resolution atmospheric reanalysis over France with the Safran system. *International journal of climatology*, *30*, 1627-1644. doi: 10.1002/joc.2003

Vogel, S. (1994). *Life in moving fluids - the physical biology of flow* (P. University, Ed.). Princeton University Press.

Wang, J., & Zhang, Z. (2019). Evaluating riparian vegetation roughness computation methods integrated within hec-ras. *Journal of Hydraulic Engineering*, *145*(6). doi: 10.1061/(ASCE)HY.1943-7900.0001597

Whittaker, P., Wilson, C., Aberle, J., Rauch, H.-P., & Xavier, P. (2013). A drag force model to incorporate the reconfiguration of full-scale riparian trees under hydrodynamic loading. *Journal of Hydraulic Research*, *51*(5), 569-580.

World Meteorological Organization. (2010). *Manual on Stream Gauging. Computation of discharge - Vol. II* (Tech. Rep. No. 1044). WMO.

Wu, F., Shen, H., & Chou, Y. (1999). Variation of roughness coefficients for unsubmerged and submerged vegetation. *Journal of hydraulic Engineering*, *125*(9), 934-942.

Yan, W., & Hunt, L.-A. (1999). An equation for modelling the temperature response of plants using only the cardinal temperatures. *Annals of Botany*, *84*, 607-614.

Yin, X., Goudriaan, J., Lantinga, E.-A., Vos, J., & Spiertz, H.-J. (2003). A flexible sigmoid function of determinate growth. *Annals of Botany*, *91*, 361-371. doi: 10.1093/aob/mcg029

Yin, X., Kropff, M.-J., McLaren, G., & Visperas, R.-M. (1995). A nonlinear model for crop development as a function of temperature. *Agricultural and Forest Meteorology*, *77*, 1-16.